10 Absorption and scattering of light in natural waters

Vladimir I. Haltrin

10.1 Introduction

In this chapter we restrict ourselves to the problems of absorption [1–13], elastic [1, 4, 5, 10, 14–22] and inelastic Raman [23–44] scattering of light, and fluorescence [45–62] in natural waters. Owing to the lack of clear and simple numerical procedures that connect scattering with easily measurable environmental parameters, scattering by air bubbles in water [63–65], Brillouin scattering [37, 66–69], and amplification of forward scattering by water turbulence [70, 71] are omitted from consideration. All conclusions of this chapter will be obtained mostly from analysis of experimental data with some additions derived from theory and from analysis of numerical computations. We will discuss in detail two basic inherent optical properties of natural water, the absorption coefficient, a, the angular scattering coefficient, β, and inelastic parameters of Raman scattering and fluorescence that are included as input parameters in a scalar radiative transfer equation:

$$\left[\frac{1}{v}\frac{\partial}{\partial t} + \mathbf{n}\nabla + c(\lambda, \boldsymbol{x})\right] L(\lambda, \boldsymbol{x}, \Omega) = Q^E(\lambda, \boldsymbol{x}, \Omega) + Q^I(\lambda, \boldsymbol{x}, \Omega), \tag{10.1}$$

here $L(\lambda, \boldsymbol{x}, \Omega)$ is a total radiance of light in water that depends on spatial coordinates $\mathbf{r}$ and time t (here $\boldsymbol{x} = (\mathbf{r}, t)$ is a combination of spatial coordinates and time), and solid angle $\Omega = \Omega(\theta, \varphi)$; v is the speed of light in water; $\mathbf{n}$ is a unit vector in the direction of propagation of light; λ is a wavelength of light; $c(\lambda, \boldsymbol{x})$ is an attenuation (or extinction) coefficient which is a sum of absorption a and beam scattering b coefficients,

$$c(\lambda, \boldsymbol{x}) = a(\lambda, \boldsymbol{x}) + b(\lambda, \boldsymbol{x}), \tag{10.2}$$

with the scattering coefficient expressed through the angular elastic scattering coefficient $\beta(\lambda, \boldsymbol{x}, \cos\vartheta)$ as follows:

$$b(\lambda, \boldsymbol{x}) = \int_{4\pi} \mathrm{d}\Omega' \beta(\lambda, \boldsymbol{x}, \cos\vartheta) \equiv 2\pi \int_0^\pi \beta(\lambda, \boldsymbol{x}, \cos\vartheta) \sin\vartheta \, \mathrm{d}\vartheta, \tag{10.3}$$

where $\cos\vartheta = \mathbf{nn}'$, $\mathbf{n}'$ is a unit vector in the direction of initial propagation of light.

The right part of eq. (10.1) consists of two source parts, elastic Q^E and inelastic Q^I.

The elastic source

$$Q^E(\lambda, \mathbf{r}, \Omega) = \int_{4\pi} \mathrm{d}\Omega' \beta(\lambda, \mathbf{r}, \cos\vartheta) L(\lambda, \mathbf{r}, \Omega'), \tag{10.4}$$

describes elastic scattering of light, *i.e.* scattering without change in wavelength.

The inelastic source

$$Q^I(\lambda, \boldsymbol{x}, \Omega) = \sum_{j=R,C,Y} \int_{\lambda'<\lambda} \mathrm{d}\lambda' \int_{4\pi} \mathrm{d}\Omega' \sigma^j(\lambda', \lambda, \boldsymbol{x}, \cos\vartheta) L(\lambda, \boldsymbol{x}, \Omega'), \tag{10.5}$$

describes an input of energy to wavelength λ from lower wavelengths λ' due to inelastic processes of Raman scattering, red fluorescence by chlorophyll, and blue fluorescence by yellow substance. Here σ^j $(j = R, C, Y)$ corresponds to Raman scattering, and chlorophyll and yellow substance emission coefficients. We ignore here anti–Stokes (blue–shifted) components that are significantly weaker than Stokes (red–shifted) components.

The previous eqs (10.1)–(10.5) introduce the following basic inherent optical properties of water:

$a(\lambda, \boldsymbol{x})$ – absorption coefficient;
$\beta(\lambda, \boldsymbol{x}, \cos\vartheta)$ – elastic angular scattering coefficient (or volume scattering function);
$\sigma^R(\lambda', \lambda, \cos\vartheta)$ – Raman scattering differential emission coefficient;
$\sigma^C(\lambda', \lambda, \boldsymbol{x}, \cos\vartheta)$ – chlorophyll fluorescence differential emission coefficient;
$\sigma^Y(\lambda', \lambda, \boldsymbol{x}, \cos\vartheta)$ – yellow substance fluorescence differential emission coefficient.

The dependence on $\boldsymbol{x}$ of all these inherent properties (except Raman scattering emission coefficient) is due to their dependence on concentrations of dissolved and suspended matter in water. Knowledge of these five basic inherent properties is enough to solve any scalar radiative transfer problem in a body of water.

Let us introduce additional four auxiliary inherent optical properties that are widely used in optics of natural waters:

elastic light scattering phase function,

$$p(\lambda, \boldsymbol{x}, \cos\vartheta) = \frac{\beta(\lambda, \boldsymbol{x}, \cos\vartheta)}{b(\lambda, \boldsymbol{x})}, \tag{10.6}$$

$$2\pi \int_0^\pi p(\lambda, \boldsymbol{x}, \cos\vartheta) \sin\vartheta \, \mathrm{d}\vartheta = 1; \tag{10.7}$$

single–scattering albedo (= probability of elastic scattering),

$$\omega_0 = \frac{b}{c} \equiv \frac{b}{a+b}; \tag{10.8}$$

backscattering coefficient,

$$b_B(\lambda, \boldsymbol{x}) = 2\pi \int_{\pi/2}^{\pi} \beta(\lambda, \boldsymbol{x}, \cos\vartheta) \sin\vartheta \, \mathrm{d}\vartheta; \tag{10.9}$$

probability of backscattering, or ratio of backscattering to scattering

$$B(\lambda, \boldsymbol{x}) = \frac{b_B(\lambda, \boldsymbol{x})}{b(\lambda, \boldsymbol{x})} = 2\pi \int_{\pi/2}^{\pi} p(\lambda, \boldsymbol{x} \cos\vartheta) \sin\vartheta \, \mathrm{d}\vartheta; \tag{10.10}$$

and Gordon's parameter,

$$x_G = \frac{b_B}{a + b_B} \equiv \frac{B\omega_0}{1 - \omega_0 + B\omega_0}. \tag{10.11}$$

Parameters ω_0, B, and x_G are dimensionless and vary in the following range for any possible type of absorbing and scattering media in natural water:

$$0 \le \omega_0 \le 1, \quad 0 \le B \le 0.5, \quad 0 \le x_G \le 1. \tag{10.12}$$

Solutions to eq. (10.1) are the basis of deriving various apparent optical properties such as diffuse attenuation coefficient, diffuse reflection coefficient, remote sensing reflection coefficient, average cosines over radiance distribution L, lidar equation, and others. In the following sections we consider inherent optical properties of natural, and mostly oceanic, water, in detail.

10.2 Absorption of light in natural water

Natural oceanic, marine or lake water consists of water molecules and impurities dissolved and suspended in water. Absorption of light occurs in water molecules, molecules of yellow substance, also known as 'Gelbstoff', dissolved organic matter (DOM), or colored dissolved organic matter (CDOM), and different kinds of chlorophyll molecules that present in phytoplankton cells that grow in natural waters. The composition of natural water is very complex and varies from region to region. In this section we restrict ourselves to a simplistic model that takes into account four major ingredients of absorption: pure water, two components of yellow substance and an average type of chlorophyll. In this approximation the absorption coefficient of natural water at wavelength of light λ at any fixed depth can be written as:

$$a(\lambda) = a_W(\lambda) + 0.06 a_C^0(\lambda) C^{0.65} + a_F^0 C_F \exp(-k_F \lambda) + a_H^0 C_H \exp(-k_H \lambda), \tag{10.13}$$

here a_W is an absorption coefficient of pure water in m^{-1}; a_C^0 is a specific absorption coefficient of chlorophyll in 1/m, and C is dimensionless concentra-

tion of chlorophyll, $C = C_C/C_0$, where C_C is a concentration of chlorophyll in $\mathrm{mg/m^3}$, and $C_0 = 1\,\mathrm{mg/m^3}$. The absorption by yellow substance or DOM is split into two parts: absorption by fulvic acid and absorption by humic acid. Both components of DOM, fulvic and humic acids, have similar optical properties with different absorption and fluorescence coefficients. For typical marine water the composition of fulvic and humic acids is, approximately, constant with $\zeta = C_H/(C_F + C_H) = 0.1$. By introducing the total concentration of DOM

$$C_Y = C_F + C_H, \tag{10.14}$$

we can rewrite eq. (10.13) in the following simplified form:

$$a(\lambda) = a_W(\lambda) + 0.06a_C^0(\lambda)C^{0.65} + a_Y^0 C_Y \exp(-k_Y\lambda). \tag{10.15}$$

The numerical values of a_W and a_C^0 are given in Table 10.1, and coefficients a_j^0 and k_j for $j = F, H, Y$ are given in Table 10.2. The spectral behavior of all absorption components is shown in Fig. 10.1.

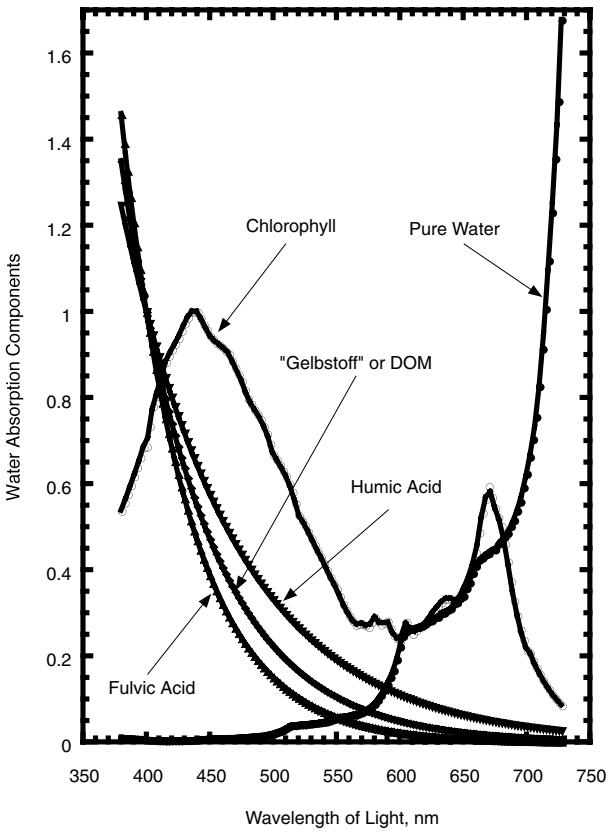

Fig. 10.1. The components of absorption of light in natural water

Table 10.1. Spectral absorption coefficient of pure water and specific spectral absorption coefficient of chlorophyll [8, 9]

λ, nm	a_w, m^{-1},	a_C^0, m^{-1}	λ, nm	a_w, m^{-1}	a_C^0, m^{-1}	λ, nm	a_w, m^{-1}	a_C^0, m^{-1}
380.0	0.01137	0.538	497.5	0.01910	0.693	615.0	0.26780	0.268
382.5	0.01044	0.557	500.0	0.02040	0.668	617.5	0.27070	0.272
385.0	0.00941	0.576	502.5	0.02280	0.657	620.0	0.27550	0.276
387.5	0.00917	0.597	505.0	0.02560	0.645	622.5	0.28100	0.287
390.0	0.00851	0.618	507.5	0.02800	0.631	625.0	0.28340	0.299
392.5	0.00829	0.639	510.0	0.03250	0.618	627.5	0.29040	0.308
395.0	0.00813	0.662	512.5	0.03720	0.600	630.0	0.29160	0.317
397.5	0.00775	0.685	515.0	0.03960	0.582	632.5	0.29950	0.325
400.0	0.00663	0.687	517.5	0.03990	0.555	635.0	0.30120	0.333
402.5	0.00579	0.734	520.0	0.04090	0.528	637.5	0.30770	0.334
405.0	0.00530	0.781	522.5	0.04160	0.516	640.0	0.31080	0.334
407.5	0.00503	0.804	525.0	0.04170	0.504	642.5	0.32200	0.330
410.0	0.00473	0.828	527.5	0.04280	0.489	645.0	0.32500	0.326
412.5	0.00452	0.855	530.0	0.04340	0.474	647.5	0.33500	0.341
415.0	0.00444	0.883	532.5	0.04470	0.459	650.0	0.34000	0.356
417.5	0.00442	0.898	535.0	0.04520	0.444	652.5	0.35800	0.372
420.0	0.00454	0.913	537.5	0.04660	0.430	655.0	0.37100	0.389
422.5	0.00474	0.926	540.0	0.04740	0.416	657.5	0.39300	0.415
425.0	0.00478	0.939	542.5	0.04890	0.400	660.0	0.41000	0.441
427.5	0.00482	0.956	545.0	0.05110	0.384	662.5	0.42400	0.488
430.0	0.00495	0.973	547.5	0.05370	0.370	665.0	0.42900	0.534
432.5	0.00504	0.987	550.0	0.05650	0.357	667.5	0.43600	0.565
435.0	0.00530	1.001	552.5	0.05930	0.339	670.0	0.43900	0.595
437.5	0.00580	1.000	555.0	0.05960	0.321	672.5	0.44800	0.570
440.0	0.00635	1.000	557.5	0.06060	0.307	675.0	0.44800	0.544
442.5	0.00696	0.986	560.0	0.06190	0.294	677.5	0.46100	0.523
445.0	0.00751	0.971	562.5	0.06400	0.283	680.0	0.46500	0.502
447.5	0.00830	0.958	565.0	0.06420	0.273	682.5	0.47800	0.461
450.0	0.00922	0.944	567.5	0.06720	0.275	685.0	0.48600	0.420
452.5	0.00969	0.936	570.0	0.06950	0.276	687.5	0.50200	0.374
455.0	0.00962	0.928	572.5	0.07330	0.272	690.0	0.51600	0.329
457.5	0.00957	0.923	575.0	0.07720	0.268	692.5	0.53800	0.295
460.0	0.00979	0.917	577.5	0.08360	0.279	695.0	0.55900	0.262
462.5	0.01005	0.909	580.0	0.08960	0.291	697.5	0.59200	0.238
465.0	0.01011	0.902	582.5	0.09890	0.282	700.0	0.62400	0.215
467.5	0.01020	0.886	585.0	0.11000	0.274	702.5	0.66300	0.208
470.0	0.01060	0.870	587.5	0.12200	0.278	705.0	0.70400	0.190
472.5	0.01090	0.855	590.0	0.13510	0.282	707.5	0.75600	0.174
475.0	0.01140	0.839	592.5	0.15160	0.265	710.0	0.82700	0.160
477.5	0.01210	0.819	595.0	0.16720	0.249	712.5	0.91400	0.146
480.0	0.01270	0.798	597.5	0.19250	0.242	715.0	1.00700	0.134
482.5	0.01310	0.786	600.0	0.22240	0.236	717.5	1.11900	0.123
485.0	0.01360	0.773	602.5	0.24700	0.258	720.0	1.23100	0.112
487.5	0.01440	0.762	605.0	0.25770	0.279	722.5	1.35600	0.103
490.0	0.01500	0.750	607.5	0.26290	0.266	725.0	1.48900	0.094
492.5	0.01620	0.734	610.0	0.26440	0.252	727.5	1.67800	0.086
495.0	0.01730	0.717	612.5	0.26650	0.260			

Table 10.2. Parameters of yellow substance ('Gelbstoff' or DOM) absorption [2]

$j \to$	$F(\zeta = 0)$	$H(\zeta = 1)$	$Y(\zeta = 0.01)$	$Y(\zeta = 0.025)$	$Y(\zeta = 0.05)$	$Y(\zeta = 0.1)$
a_j^0, $\mathrm{m^2\,mg}$	35.959	18.828	14.547	8.5472	6.2777	5.6797
k_j, $\mathrm{nm^{-1}}$	0.0189	0.011 05	0.016 58	0.014 96	0.013 69	0.012 62

10.3 Elastic scattering of light in natural water

The light propagating in natural water elastically scatters on density fluctuations of water molecules (Rayleigh scattering) and any kind of physical inhomogeneity that is larger than the water molecule (Mie scattering). Such inhomogeneities consist of any kind of suspended organic and terrigenic living or dead particles. Terrigenic particles consist of small fractions of mineral origin that can be found in any region of open ocean as well as in coastal areas of seas and in lakes; shallow coastal areas also contain terrigenic fractions related to clays and suspended quartz particles. Organic particles consist of living particles such as bacteria [72–74], zooplankton and phytoplankton, and dead particles such as detritus and zooplankton feces with predominant abundance of phytoplankton cells. In this paragraph we consider Rayleigh scattering by pure water, and experimentally measured volume scattering functions.

The elastic angular scattering coefficient and total elastic scattering coefficient can be expressed as a sum of coefficients due to water molecules and particular matter that consists of phytoplankton cells, detritus, bacteria, suspended terrigenic particles of mineral origin, suspended clay particles, quartz particles, etc.,

$$\beta(\lambda, \cos\vartheta) = \beta_W(\lambda, \cos\vartheta) + \beta_P(\lambda, \cos\vartheta), \quad b(\lambda) = b_W(\lambda) + b_P(\lambda). \tag{10.16}$$

The particulate part depends on the concentration of suspended particles and will be presented here in the tabular form of experimentally measured data and in the form of experimentally derived optical models.

10.3.1 Rayleigh scattering in pure water

According to Morel [15] the pure water angular scattering coefficient may be represented as:

$$\beta_W(\lambda, \vartheta) = b_W(\lambda) p_W(\cos\vartheta), \tag{10.17}$$

where

$$b_W(\lambda) = (0.001\,458\,4\,\mathrm{m^{-1}}) \left(\frac{550}{\lambda}\right)^{4.34}, \tag{10.18}$$

is a total natural base scattering coefficient of pure marine water with average salinity, temperature $T = 20°\mathrm{C}$, and depolarization factor $\delta = 0.09$. The wavelength λ in eq. (10.18) is in nm.

The normalized according to eq. (10.7) phase function of scattering of pure water that takes into account the depolarization effects with $\delta = 0.09$ is:

$$p_W(\cos\vartheta) = 0.062\,253\,2 + 0.051\,972\,8\cos^2\vartheta \tag{10.19}$$

10.3.2 Petzold experimental volume scattering functions

For almost three decades of the last century the experimental database of 15 angular scattering coefficients (ASC) β published by Petzold [75] was used by ocean optics scientific community. These VSF have been measured with the angular scattering meter with maximum sensitivity centered at 515 nm and with the half-width of sensitivity about 60 nm. The waters that were used to measure these angular scattering coefficients were taken in the coastal areas of the Pacific Ocean near the shares of Southern California. The ranges of variability of integral inherent optical properties were: $0.093\,\mathrm{m}^{-1} \le c \le 2.19\,\mathrm{m}^{-1}$; $0.008\,\mathrm{m}^{-1} \le b \le 1.824\,\mathrm{m}^{-1}$; $0.082\,\mathrm{m}^{-1} \le a \le 0.764\,\mathrm{m}^{-1}$; $0.091 \le \omega_0 \le 0.906$; $0.013 \le B \le 0.146$. The actual values of Petzold angular scattering coefficients with corresponding inherent optical properties are given in Tables 10.3 and 10.4.

10.3.3 Mankovsky experimental volume scattering functions

More recently another 41 volume scattering functions with associated attenuation and beam scattering coefficients that have been measured in natural waters of the Atlantic, Indian and Southern Oceans, the Mediterranean and Black Seas, and Lake Baikal were published by Mankovsky and Haltrin [76, 77]. These phase functions have been measured with a nephelometer (an angular scattering meter) that has a maximum of sensitivity at 520 nm with the half-width of sensitivity band about 40 nm. The ranges of variability of integral inherent optical properties were: $0.115\,\mathrm{m}^{-1} \le c \le 1.105\,\mathrm{m}^{-1}$; $0.000\,143\,\mathrm{m}^{-1} \le b \le 0.0103\,\mathrm{m}^{-1}$; $0.021\,\mathrm{m}^{-1} \le a \le 0.163\,\mathrm{m}^{-1}$; $0.435 \le \omega_0 \le 0.867$; $0.0078 \le B \le 0.037$. The angular scattering coefficients and corresponding inherent optical properties are given in Tables 10.5 and 10.6.

10.3.4 Lee experimental volume scattering functions

During the period between 2000 and 2004 more than a thousand high-resolution angular light scattering coefficients of marine water have been measured with the polar nephelometer that was developed and assembled by Michael E. Lee. The maximum intensity of this nephelometer was centered at 550 nm. The complete set of technical parameters of this probe was published in Haltrin *et al.*, [78] and Lee and Lewis [79]. The modified version of this nephelometer that has the ability to measure angular scattering coefficients at six wavelengths (443, 490, 510, 555, 590, and 620 nm) was developed and tested in 2003 by M. E. Lee in waters of Mobile Bay in the Gulf of Mexico. Some of the results of these measurements are presented in this section.

The measurements of more than 60 angular scattering coefficients [80] have been accomplished in 2000 in coastal waters near the shores of New Jersey in

Table 10.3a. Petzold [75] total angular scattering functions in m^{-1} $ster^{-1}$ (cases 1-8)

angle, $^\circ$	β_{01}	β_{02}	β_{03}	β_{04}	β_{05}	β_{06}	β_{07}	β_{08}
0.1	355.78	53.182	75.181	871.25	653.290	2689.7	3262.0	2215.3
0.169	153.72	28.464	39.059	387.01	290.350	1396.9	1609.8	1039.7
0.338	50.739	12.465	16.446	132.49	99.4720	585.05	618.23	395.09
0.573	20.348	5.9045	7.3639	57.757	43.2250	283.71	307.91	184.58
1.72	2.9015	1.0191	1.1855	8.1372	6.29410	49.063	54.684	34.040
5.73	2.9564e-01	1.1347e-01	1.2633e-01	7.3434e-01	6.32420e-01	5.1290	5.9699	4.3004
10	9.9395e-02	4.1620e-02	4.4602e-02	2.4154e-01	2.15540e-01	1.7321	2.1107	1.4749
15	4.7716e-02	2.0375e-02	2.0871e-02	1.0703e-01	9.28280e-02	7.7653e-01	9.0405e-01	5.9012e-01
20	2.6227e-02	1.0990e-02	1.1988e-02	5.4145e-02	4.42680e-02	3.9389e-01	4.4523e-01	2.9443e-01
25	1.5466e-02	6.1656e-03	7.0743e-03	3.0441e-02	2.39000e-02	2.4745e-01	2.7335e-01	1.6615e-01
30	9.7519e-03	3.8877e-03	4.2671e-03	1.7026e-02	1.44500e-02	1.3752e-01	1.6128e-01	1.0204e-01
40	4.6734e-03	1.8991e-03	1.9990e-03	7.2160e-03	6.01400e-03	6.8674e-02	7.9133e-02	4.8882e-02
50	2.3972e-03	1.0196e-03	1.0695e-03	3.8094e-03	2.99340e-03	3.7004e-02	4.3884e-02	2.5982e-02
60	1.4785e-03	6.0280e-04	6.4576e-04	2.1547e-03	1.73660e-03	2.1594e-02	2.5483e-02	1.4840e-02
70	9.9904e-04	4.0688e-04	4.3685e-04	1.3769e-03	1.09400e-03	1.4017e-02	1.6550e-02	9.6046e-03
80	7.0735e-04	3.0191e-04	3.0890e-04	9.3400e-04	7.23760e-04	9.7490e-03	1.1239e-02	6.7265e-03
90	5.3652e-04	2.4593e-04	2.4592e-04	7.1848e-04	5.24120e-04	7.2413e-03	8.4110e-03	4.8646e-03
100	4.6757e-04	2.2394e-04	2.1893e-04	5.7577e-04	4.36260e-04	5.6499e-03	6.6940e-03	3.9923e-03
110	4.4657e-04	2.2393e-04	2.1892e-04	5.1384e-04	4.07270e-04	4.7480e-03	5.8912e-03	3.4458e-03
120	4.2656e-04	2.3392e-04	2.2891e-04	4.9379e-04	3.97230e-04	4.3681e-03	5.5491e-03	3.1757e-03
130	4.3649e-04	2.6290e-04	2.5689e-04	5.1058e-04	4.07100e-04	4.1531e-03	5.1541e-03	2.8847e-03
140	4.3638e-04	2.7488e-04	2.7486e-04	5.7309e-04	4.45820e-04	3.9046e-03	4.8223e-03	2.8087e-03
150	4.8909e-04	3.0882e-04	3.0180e-04	6.6212e-04	5.23190e-04	4.1061e-03	4.6344e-03	2.9532e-03
160	5.7340e-04	3.6268e-04	3.4665e-04	8.0075e-04	6.66510e-04	4.6227e-03	5.1417e-03	3.3427e-03
170	7.5441e-04	4.6710e-04	4.6697e-04	1.2964e-03	9.39270e-04	5.8137e-03	5.5497e-03	3.5323e-03
a, m^{-1}	0.082	0.114	0.122	0.195	0.179	0.337	0.366	0.125
b, m^{-1}	0.117	0.037	0.043	0.275	0.219	1.583	1.824	1.205
b_B, m^{-1}	0.002 92	0.001 63	0.001 63	0.003 85	0.002 85	0.0301	0.0365	0.0212
$\omega_0 = b/c$	0.588	0.247	0.258	0.585	0.551	0.824	0.833	0.906
$B = b_B/b$	0.025	0.044	0.038	0.014	0.013	0.019	0.020	0.018

Table 10.3b. Petzold [75] total angular scattering functions in m^{-1} $ster^{-1}$ (cases 9-15)

angle, °	β_{09}	β_{10}	β_{11}	β_{12}	β_{13}	β_{14}	β_{15}
0.1	2.3282	179.35	199.01	1356.7	843.35	185.95	1.8806
0.169	1.6820	133.13	144.74	873.28	440.53	92.305	—
0.338	1.0948	74.022	78.744	429.80	186.82	36.595	0.47797
0.573	6.9716e-01	44.265	46.846	230.23	83.938	15.455	—
1.72	1.8949e-01	14.547	15.277	47.846	12.466	2.4432	7.6815e-02
5.73	3.0964e-02	2.8018	3.0244	4.7692	1.2830	2.4749e-01	—
10	1.2294e-02	9.1763e-01	9.5995e-01	1.4783	4.4257e-01	7.5584e-02	1.1095e-02
15	5.9282e-03	3.2706e-01	3.5423e-01	5.3683e-01	1.7070e-01	3.3611e-02	7.3780e-03
20	3.2493e-03	1.6484e-01	1.6867e-01	2.9776e-01	9.8342e-02	1.9562e-02	4.6391e-03
25	1.8397e-03	8.6398e-02	8.5362e-02	1.6590e-01	5.1004e-02	1.0484e-02	2.1897e-03
30	1.1498e-03	5.2544e-02	5.1529e-02	1.0681e-01	3.5173e-02	6.7314e-03	1.1299e-03
40	5.2494e-04	2.1259e-02	2.1947e-02	5.2872e-02	1.6021e-02	2.8472e-03	5.8194e-04
50	3.1297e-04	1.1337e-02	1.0936e-02	2.6257e-02	8.3755e-03	1.5787e-03	3.6297e-04
60	2.2398e-04	6.0804e-03	5.8599e-03	1.4335e-02	4.7229e-03	9.0335e-04	2.6098e-04
70	1.8299e-04	3.7631e-03	3.4636e-03	8.9651e-03	2.8505e-03	5.8462e-04	2.0999e-04
80	1.6099e-04	2.4595e-03	2.4291e-03	5.9897e-03	1.9039e-03	4.1874e-04	1.8899e-04
90	1.4699e-04	1.8223e-03	1.8916e-03	4.4557e-03	1.4554e-03	3.3579e-04	1.6499e-04
100	1.4399e-04	1.5633e-03	1.5630e-03	3.3661e-03	1.1862e-03	2.9282e-04	1.5899e-04
110	1.5399e-04	1.4136e-03	1.4631e-03	2.9983e-03	1.0764e-03	2.8581e-04	1.6499e-04
120	1.6599e-04	1.4231e-03	1.3929e-03	2.8275e-03	1.0053e-03	2.9579e-04	1.7599e-04
130	1.8398e-04	1.4420e-03	1.4416e-03	2.7146e-03	9.7299e-04	3.0875e-04	2.0198e-04
140	1.9698e-04	1.5398e-03	1.4499e-03	2.7076e-03	9.7220e-04	3.2668e-04	2.2598e-04
150	2.1597e-04	1.6656e-03	1.5657e-03	2.7242e-03	1.0035e-03	3.6154e-04	2.5097e-04
160	2.5794e-04	1.7669e-03	1.7459e-03	2.9776e-03	1.1587e-03	4.0822e-04	2.6995e-04
170	3.2384e-04	2.4399e-03	2.2033e-03	3.3589e-03	1.4491e-03	4.9891e-04	3.5085e-04
a, m^{-1}	0.093	0.138	0.764	0.196	0.188	0.093	0.085
b, m^{-1}	0.009	0.547	0.576	1.284	0.407	0.081	0.008
b_B, m^{-1}	0.00107	0.00984	0.00979	0.0193	0.00692	0.00203	0.00117
$\omega_0 = b/c$	0.093	0.798	0.430	0.867	0.685	0.463	0.091
$B = b_B/b$	0.119	0.018	0.017	0.015	0.017	0.025	0.146

Table 10.4. Additional inherent optical properties to 15 Petzold angular scattering coefficients [75]. Maximal values of these properties are printed in bold and minimum values are printed in bold italic

#	c, m^{-1}	b, m^{-1}	a, m^{-1}	b_B, m^{-1}	$\omega_0 = b/c$	$B = b_B/b$	$x_G = b_B/(a+b_B)$	$\beta(140^\circ)$, $m^{-1}\,ster^{-1}$	$p(140^\circ)$, $ster^{-1}$
1	0.199	0.117	***0.082***	0.002 925	0.588	0.025	0.034 442	0.000 436 38	0.003 729 7
2	0.151	0.037	0.114	0.001 628	0.247	0.044	0.014 080	0.000 274 88	0.007 429 2
3	0.165	0.043	0.122	0.001 634	0.258	0.038	0.013 216	0.000 274 86	0.006 392 1
4	0.470	0.275	0.195	0.003 850	0.585	0.014	0.019 361	0.000 573 09	0.002 084 0
5	0.398	0.219	0.179	0.002 847	0.551	***0.013***	0.015 656	0.000 445 82	***0.002 035 7***
6	1.920	1.583	0.337	0.030 077	0.824	0.019	0.081 936	0.003 904 60	0.002 466 6
7	**2.190**	**1.824**	0.366	**0.036 480**	0.833	0.020	0.090 638	**0.004 822 30**	0.002 643 8
8	1.330	1.205	0.125	0.021 690	**0.906**	0.018	**0.147 860**	0.002 808 70	0.002 330 9
9	0.102	0.009	0.093	***0.001 071***	0.093	0.119	***0.011 385***	***0.000 196 98***	0.021 887 0
10	0.685	0.547	0.138	0.009 846	0.798	0.018	0.066 596	0.001 539 80	0.002 815 0
11	1.340	0.576	0.764	0.009 792	0.430	0.017	0.012 655	0.001 449 90	0.002 517 2
12	1.480	1.284	0.196	0.019 260	0.867	0.015	0.089 473	0.002 707 60	0.002 108 7
13	0.595	0.407	0.188	0.006 919	0.685	0.017	0.035 497	0.000 972 20	0.002 388 7
14	0.174	0.081	0.093	0.002 025	0.463	0.025	0.021 310	0.000 326 68	0.004 033 1
15	***0.093***	***0.008***	0.085	0.001 168	***0.091***	**0.146**	0.013 555	0.000 225 98	**0.028 247 0**

Table 10.5a. Mankovsky [76, 77] seawater angular scattering coefficients in $m^{-1}\,ster^{-1}$ (cases 1–7). Values in parentheses represent extrapolated and interpolated values

ang, °	β_{01}	β_{02}	β_{03}	β_{04}	β_{05}	β_{06}	β_{07}
(0.25)	146.29	56.691	32.871	57.838	23.036	43.313	22.265
(0.75)	85.333	36.418	20.961	28.243	12.411	32.249	16.673
(1.25)	50.982	23.884	13.640	14.313	6.9058	24.278	12.630
(1.50)	39.757	19.490	11.090	10.333	5.2133	21.150	11.041
(1.75)	31.197	15.985	9.0618	7.5304	3.9675	18.476	9.6787
2.0	24.267	13.032	7.3285	5.4327	2.9855	16.033	8.4143
(2.5)	15.621	9.0974	5.0994	3.0833	1.8362	12.520	6.6300
(3.5)	6.7564	4.6102	2.5452	1.0684	0.73573	7.7413	4.1669
(4.5)	3.2175	2.5352	1.3792	0.43005	0.33529	4.9982	2.7404
(5.5)	1.6866	1.5136	0.81155	0.20106	0.17387	3.3707	1.8863
(6.5)	0.97323	0.98088	0.51822	0.10915	0.10257	2.3742	1.3587
7.5	0.47634	0.55965	0.26786	0.45490E-01	0.45490E-01	1.5063	0.84706
12.5	0.12809	0.22260	0.84628E-01	0.19387E-01	0.19387E-01	0.47590	0.28676
(15.0)	0.97480E-01	0.14754	0.64404E-01	0.14925E-01	0.14925E-01	0.31183	0.17944
17.5	0.74185E-01	0.97795E-01	0.49013E-01	0.11490E-01	0.11490E-01	0.20432	0.11228
22.5	0.29855E-01	0.49547E-01	0.23715E-01	0.71617E-02	0.76739E-02	0.12735	0.73285E-01
27.5	0.21214E-01	0.32856E-01	0.13697E-01	0.42327E-02	0.47491E-02	0.62606E-01	0.44322E-01
(30.0)	0.16388E-01	0.23416E-01	0.10340E-01	0.37112E-02	0.39311E-02	0.53029E-01	0.31953E-01
32.5	0.12659E-01	0.16688E-01	0.78058E-02	0.32540E-02	0.32540E-02	0.44918E-01	0.23036E-01
37.5	0.96965E-02	0.14342E-01	0.43313E-02	0.22213E-02	0.22213E-02	0.21708E-01	0.13385E-01
42.5	0.36468E-02	0.76193E-02	0.39987E-02	0.15557E-02	0.17455E-02	0.21474E-01	0.87481E-02
(45.0)	0.29574E-02	0.59692E-02	0.29917E-02	0.13675E-02	0.13993E-02	0.13518E-01	0.71765E-02
47.5	0.23978E-02	0.46754E-02	0.22378E-02	0.12018E-02	0.11215E-02	0.85078E-02	0.58859E-02
52.5	0.17853E-02	0.32487E-02	0.16282E-02	0.89478E-03	0.89478E-03	0.59117E-02	0.43824E-02
57.5	0.12252E-02	0.24446E-02	0.13747E-02	0.70504E-03	0.70504E-03	0.43473E-02	0.30776E-02
62.5	0.93350E-03	0.16987E-02	0.10236E-02	0.51300E-03	0.57559E-03	0.34683E-02	0.21385E-02
67.5	0.64242E-03	0.15410E-02	0.10661E-02	0.47623E-03	0.47623E-03	0.24993E-02	0.20788E-02
72.5	0.55159E-03	0.11524E-02	0.77914E-03	0.39050E-03	0.39050E-03	0.17849E-02	0.14178E-02
77.5	0.44855E-03	0.89498E-03	0.56470E-03	0.35630E-03	0.35630E-03	0.15915E-02	0.11267E-02
82.5	0.39675E-03	0.90890E-03	0.49948E-03	0.28088E-03	0.28088E-03	0.13757E-02	0.11442E-02
87.5	0.36460E-03	0.69473E-03	0.57785E-03	0.25812E-03	0.28302E-03	0.13862E-02	0.91583E-03
(90.0)	0.37309E-03	0.61918E-03	0.49753E-03	0.25663E-03	0.28139E-03	0.12213E-02	0.91583E-03
92.5	0.38178E-03	0.55184E-03	0.42837E-03	0.25516E-03	0.27978E-03	0.10760E-02	0.91583E-03
97.5	0.36184E-03	0.62880E-03	0.40599E-03	0.27702E-03	0.27702E-03	0.99659E-03	0.99659E-03
102.5	0.33252E-03	0.57785E-03	0.37309E-03	0.27153E-03	0.27153E-03	0.98133E-03	0.67892E-03
107.5	0.34803E-03	0.60481E-03	0.38161E-03	0.26462E-03	0.29690E-03	0.10271E-02	0.79729E-03
112.5	0.39611E-03	0.54678E-03	0.34500E-03	0.28630E-03	0.28630E-03	0.97233E-03	0.68836E-03
117.5	0.34683E-03	0.54969E-03	0.43663E-03	0.31413E-03	0.31413E-03	0.91225E-03	0.70813E-03
122.5	0.41516E-03	0.62837E-03	0.42483E-03	0.33282E-03	0.33282E-03	0.90827E-03	0.72147E-03
127.5	0.46959E-03	0.64821E-03	0.45890E-03	0.34891E-03	0.34891E-03	0.10040E-02	0.91562E-03
132.5	0.54931E-03	0.63069E-03	0.48957E-03	0.40347E-03	0.35960E-03	0.10711E-02	0.91162E-03
137.5	0.59145E-03	0.69489E-03	0.50340E-03	0.40918E-03	0.45911E-03	0.11013E-02	0.10278E-02
(140)	0.64695E-03	0.74153E-03	0.50035E-03	0.43718E-03	0.46214E-03	0.11203E-02	0.11243E-02
142.5	0.70245E-03	0.78816E-03	0.49730E-03	0.46517E-03	0.46517E-03	0.11392E-02	0.12207E-02
147.5	0.74545E-03	0.85589E-03	0.55261E-03	0.48800E-03	0.48800E-03	0.12371E-02	0.10775E-02
152.5	0.70245E-03	0.82531E-03	0.36026E-03	0.53532E-03	0.53532E-03	0.13385E-02	0.12207E-02
157.5	0.96609E-03	0.11092E-02	0.50701E-03	0.58886E-03	0.58886E-03	0.20184E-02	0.13336E-02
162.5	0.10723E-02	0.11758E-02	0.56275E-03	0.57586E-03	0.61704E-03	0.20432E-02	0.15860E-02

Table 10.5b. Mankovsky [76, 77] seawater angular scattering coefficients in $m^{-1}\,ster^{-1}$ (cases 8–14). Values in parentheses represent extrapolated and interpolated values.

ang, °	β_{08}	β_{09}	β_{10}	β_{11}	β_{12}	β_{13}	β_{14}
(0.25)	105.37	53.545	42.026	163.01	93.372	46.485	51.345
(0.75)	64.926	30.684	21.848	104.76	57.308	28.213	31.941
(1.25)	40.928	18.023	11.787	68.741	35.910	17.523	20.315
(1.50)	32.765	13.961	8.7804	56.133	28.656	13.929	16.335
(1.75)	26.382	10.890	6.6026	46.049	23.026	11.137	13.209
2.0	21.136	8.4143	4.9547	37.602	18.417	8.8112	10.593
(2.5)	14.240	5.3817	2.9670	26.074	12.366	5.8919	7.2180
(3.5)	6.7720	2.3121	1.1634	13.098	5.8373	2.7329	3.4840
(4.5)	3.5238	1.1074	0.52944	7.0993	3.0284	1.3901	1.8370
(5.5)	2.0064	0.59104	0.27952	4.1612	1.7227	0.77535	1.0581
(6.5)	1.2497	0.35157	0.17128	2.6255	1.0721	0.47424	0.66580
7.5	0.70456	0.16901	0.92879E-01	1.5784	0.58643	0.23330	0.35311
12.50	0.28023	0.59926E-01	0.87502E-01	0.58508	0.24390	0.70397E-01	0.12519
(15.0)	0.19450	0.42074E-01	0.47744E-01	0.45626	0.18587	0.47748E-01	0.86887E-01
17.5	0.13499	0.29540E-01	0.24571E-01	0.35499	0.14132	0.32386E-01	0.60306E-01
22.5	0.62376E-01	0.15672E-01	0.13336E-01	0.19734	0.55618E-01	0.18839E-01	0.31265E-01
27.5	0.30663E-01	0.10392E-01	0.86420E-02	0.96876E-01	0.27939E-01	0.10390E-01	0.14676E-01
(30.0)	0.24804E-01	0.84065E-02	0.67533E-02	0.74854E-01	0.22091E-01	0.88009E-02	0.11469E-01
32.5	0.20064E-01	0.68001E-02	0.52773E-02	0.57838E-01	0.17467E-01	0.74547E-02	0.89626E-02
37.5	0.14676E-01	0.41373E-02	0.37733E-02	0.40385E-01	0.11123E-01	0.41368E-02	0.59795E-02
42.5	0.98156E-02	0.34827E-02	0.27034E-02	0.34058E-01	0.79839E-02	0.31038E-02	0.41870E-02
(45.0)	0.88291E-02	0.27920E-02	0.21425E-02	0.28590E-01	0.65496E-02	0.24596E-02	0.35146E-02
47.5	0.79399E-02	0.22383E-02	0.16975E-02	0.24000E-01	0.53730E-02	0.19492E-02	0.29502E-02
52.5	0.64821E-02	0.18269E-02	0.13235E-02	0.14495E-01	0.40852E-02	0.17048E-02	0.20974E-02
57.5	0.42483E-02	0.14071E-02	0.10674E-02	0.12538E-01	0.30776E-02	0.14068E-02	0.16529E-02
62.5	0.30911E-02	0.11226E-02	0.10003E-02	0.85156E-02	0.22398E-02	0.11224E-02	0.12593E-02
67.5	0.25575E-02	0.10421E-02	0.88678E-03	0.60009E-02	0.18976E-02	0.10419E-02	0.10419E-02
72.5	0.19571E-02	0.79747E-03	0.59104E-03	0.39014E-02	0.12625E-02	0.79732E-03	0.91545E-03
77.5	0.15553E-02	0.71091E-03	0.60508E-03	0.35663E-02	0.12948E-02	0.81620E-03	0.81620E-03
82.5	0.11709E-02	0.61449E-03	0.48811E-03	0.25016E-02	0.11434E-02	0.61445E-03	0.72191E-03
87.5	0.98133E-03	0.52701E-03	0.49183E-03	0.23026E-02	0.10285E-02	0.61916E-03	0.61916E-03
(90.0)	0.89498E-03	0.51798E-03	0.48341E-03	0.21243E-02	0.94889E-03	0.56144E-03	0.56144E-03
92.5	0.81624E-03	0.50911E-03	0.47513E-03	0.19598E-02	0.87542E-03	0.50910E-03	0.50910E-03
97.5	0.79162E-03	0.57348E-03	0.45553E-03	0.18976E-02	0.84765E-03	0.57343E-03	0.57343E-03
102.5	0.76176E-03	0.46432E-03	0.30677E-03	0.18290E-02	0.81699E-03	0.46430E-03	0.46430E-03
107.5	0.64806E-03	0.43323E-03	0.28616E-03	0.14833E-02	0.77842E-03	0.43315E-03	0.50890E-03
112.5	0.68836E-03	0.40079E-03	0.37395E-03	0.16528E-02	0.73827E-03	0.37396E-03	0.40071E-03
117.5	0.64583E-03	0.43173E-03	0.34286E-03	0.17387E-02	0.77663E-03	0.43166E-03	0.43166E-03
122.5	0.67331E-03	0.38754E-03	0.32985E-03	0.15784E-02	0.99590E-03	0.45524E-03	0.45524E-03
127.5	0.72730E-03	0.40431E-03	0.34412E-03	0.14165E-02	0.89375E-03	0.46418E-03	0.46418E-03
132.5	0.70765E-03	0.46764E-03	0.35466E-03	0.15143E-02	0.91246E-03	0.35469E-03	0.46757E-03
137.5	0.69489E-03	0.39987E-03	0.39987E-03	0.15930E-02	0.89581E-03	0.39985E-03	0.46978E-03
(140)	0.76971E-03	0.42159E-03	0.39749E-03	0.16004E-02	0.95511E-03	0.36805E-03	0.48357E-03
142.5	0.84453E-03	0.44332E-03	0.39511E-03	0.16077E-02	0.10144E-02	0.33625E-03	0.49735E-03
147.5	0.74545E-03	0.48141E-03	0.40965E-03	0.17467E-02	0.98224E-03	0.36512E-03	0.48132E-03
152.5	0.86420E-03	0.52085E-03	0.48598E-03	0.18459E-02	0.88352E-03	0.48598E-03	0.48598E-03
157.5	0.96609E-03	0.66852E-03	0.58212E-03	0.23726E-02	0.94453E-03	0.44163E-03	0.58218E-03
162.5	0.91267E-03	0.75930E-03	0.69233E-03	0.21888E-02	0.11226E-02	0.57591E-03	0.69240E-03

Table 10.5c. Mankovsky [76, 77] seawater angular scattering coefficients in $m^{-1}\,ster^{-1}$ (cases 15–21). Values in parentheses represent extrapolated and interpolated values

ang, °	β_{15}	β_{16}	β_{17}	β_{18}	β_{19}	β_{20}	β_{21}
(0.25)	30.802	41.392	30.303	29.081	34.223	29.211	78.944
(0.75)	16.977	22.554	19.393	17.419	22.874	18.136	44.589
(1.25)	9.6529	12.675	12.667	10.699	15.537	11.509	25.892
(1.50)	7.3643	9.6121	10.316	8.4637	12.882	9.2443	19.936
(1.75)	5.6622	7.3460	8.4441	6.7377	10.724	7.4656	15.457
2.0	4.3156	5.5595	6.8397	5.3093	8.8112	5.9571	11.886
(2.5)	2.6967	3.4345	4.7748	3.5294	6.3388	4.0636	7.5090
(3.5)	1.1185	1.3884	2.3978	1.6270	3.3267	1.9498	3.1594
(4.5)	0.52549	0.63503	1.3063	0.82909	1.8622	1.0212	1.4849
(5.5)	0.27963	0.32862	0.77216	0.46705	1.1117	0.58376	0.77958
(6.5)	0.16854	0.19240	0.49517	0.29084	0.70792	0.36426	0.45720
7.5	0.80894E-01	0.88698E-01	0.25581	0.14385	0.35311	0.17698	0.22280
12.5	0.39587E-01	0.36104E-01	0.80826E-01	0.53401E-01	0.75431E-01	0.50998E-01	0.80826E-01
(15.0)	0.27794E-01	0.28116E-01	0.58071E-01	0.37928E-01	0.53574E-01	0.38811E-01	0.52961E-01
17.5	0.19515E-01	0.21896E-01	0.41721E-01	0.26938E-01	0.38050E-01	0.29536E-01	0.34702E-01
22.5	0.12163E-01	0.10841E-01	0.24835E-01	0.17581E-01	0.21138E-01	0.17581E-01	0.17581E-01
27.5	0.70246E-02	0.94759E-02	0.14676E-01	0.94759E-02	0.94759E-02	0.10390E-01	0.94759E-02
(30.0)	0.57481E-02	0.70717E-02	0.10953E-01	0.75775E-02	0.80265E-02	0.88009E-02	0.75775E-02
32.5	0.47036E-02	0.52776E-02	0.81740E-02	0.60594E-02	0.67988E-02	0.74547E-02	0.60594E-02
37.5	0.31381E-02	0.37728E-02	0.59795E-02	0.35210E-02	0.47497E-02	0.47497E-02	0.37728E-02
42.5	0.23545E-02	0.23545E-02	0.34826E-02	0.31038E-02	0.34826E-02	0.34826E-02	0.23545E-02
(45.0)	0.19993E-02	0.21423E-02	0.34346E-02	0.24596E-02	0.27917E-02	0.29914E-02	0.19993E-02
47.5	0.16976E-02	0.19492E-02	0.33872E-02	0.19492E-02	0.22379E-02	0.25695E-02	0.16976E-02
52.5	0.13234E-02	0.15548E-02	0.18268E-02	0.18268E-02	0.17048E-02	0.18268E-02	0.15548E-02
57.5	0.10672E-02	0.11974E-02	0.18124E-02	0.16529E-02	0.18124E-02	0.16529E-02	0.14068E-02
62.5	0.10003E-02	0.11224E-02	0.17384E-02	0.12593E-02	0.14796E-02	0.12593E-02	0.85142E-03
67.5	0.77238E-03	0.88681E-03	0.15411E-02	0.11690E-02	0.13117E-02	0.10419E-02	0.77238E-03
72.5	0.59106E-03	0.69444E-03	0.10756E-02	0.91545E-03	0.10756E-02	0.91545E-03	0.59106E-03
77.5	0.51499E-03	0.60506E-03	0.93712E-03	0.71088E-03	0.71088E-03	0.71088E-03	0.51499E-03
82.5	0.52298E-03	0.52298E-03	0.82886E-03	0.61445E-03	0.61445E-03	0.52298E-03	0.52298E-03
87.5	0.49181E-03	0.52699E-03	0.72745E-03	0.52699E-03	0.52699E-03	0.52699E-03	0.49181E-03
(90.0)	0.48339E-03	0.51797E-03	0.65963E-03	0.56144E-03	0.56144E-03	0.56144E-03	0.40673E-03
92.5	0.47512E-03	0.50910E-03	0.59814E-03	0.59814E-03	0.59814E-03	0.59814E-03	0.33636E-03
97.5	0.45550E-03	0.48807E-03	0.48807E-03	0.57343E-03	0.67373E-03	0.48807E-03	0.45550E-03
102.5	0.46430E-03	0.46430E-03	0.43331E-03	0.64091E-03	0.46430E-03	0.46430E-03	0.43331E-03
107.5	0.40424E-03	0.43315E-03	0.40424E-03	0.43315E-03	0.43315E-03	0.43315E-03	0.40424E-03
112.5	0.40071E-03	0.37396E-03	0.40071E-03	0.47079E-03	0.55313E-03	0.47079E-03	0.37396E-03
117.5	0.36740E-03	0.43166E-03	0.43166E-03	0.58230E-03	0.50716E-03	0.36740E-03	0.36740E-03
122.5	0.38748E-03	0.45524E-03	0.45524E-03	0.60013E-03	0.45524E-03	0.45524E-03	0.38748E-03
127.5	0.40428E-03	0.46418E-03	0.40428E-03	0.62616E-03	0.40428E-03	0.46418E-03	0.40428E-03
132.5	0.40724E-03	0.40724E-03	0.40724E-03	0.46757E-03	0.46757E-03	0.40724E-03	0.35469E-03
137.5	0.39985E-03	0.39985E-03	0.39985E-03	0.46978E-03	0.46978E-03	0.39985E-03	0.39985E-03
(140.0)	0.42156E-03	0.44860E-03	0.44860E-03	0.48357E-03	0.45652E-03	0.42156E-03	0.39746E-03
142.5	0.44326E-03	0.49735E-03	0.49735E-03	0.49735E-03	0.44326E-03	0.44326E-03	0.39506E-03
147.5	0.40967E-03	0.56550E-03	0.56550E-03	0.48132E-03	0.40967E-03	0.48132E-03	0.48132E-03
152.5	0.44322E-03	0.59789E-03	0.48598E-03	0.52074E-03	0.44322E-03	0.52074E-03	0.44322E-03
157.5	0.38464E-03	0.66843E-03	0.38464E-03	0.86110E-03	0.58218E-03	0.76746E-03	0.50706E-03
162.5	0.51328E-03	0.87168E-03	0.57591E-03	0.64619E-03	0.64619E-03	0.97804E-03	0.64619E-03

Table 10.6. Additional inherent optical properties to 21 Mankovsky angular scattering coefficients [76, 77]. Maximal values of these properties are printed in bold and minimum values are printed in bold italic

#	c, m^{-1}	b, m^{-1}	a, m^{-1}	b_B, m^{-1}	$\omega_0 = b/c$	$B = b_B/b$	$x_G = b_B/(a+b_B)$	$\beta(140°)$, $m^{-1}\,ster^{-1}$	$p(140°)$, $ster^{-1}$
1	0.557 23	0.409 86	0.147 37	0.001 312 4	0.735 53	***0.007 813***	0.021 266	0.646 949E-03	***0.157 846E-02***
2	0.402 95	0.299 34	0.103 61	0.001 280 1	0.742 87	0.014 286	0.039 638	0.741 526E-03	0.247 720E-02
3	0.276 31	0.156 58	0.119 73	0.000 437 8	0.566 68	0.017 857	0.022 820	0.500 350E-03	0.319 549E-02
4	0.161 18	0.105 92	0.055 26	0.000 238 7	0.657 15	0.021 277	0.039 185	0.437 178E-03	0.412 743E-02
5	0.142 76	***0.062 17***	0.080 59	***0.000 143 2***	***0.435 49***	**0.037 037**	0.027 778	0.462 142E-03	**0.743 351E-02**
6	0.626 30	0.518 08	0.108 22	0.003 676 9	0.827 21	0.013 699	0.061 545	0.112 028E-02	0.216 238E-02
7	0.435 19	0.290 13	0.145 06	0.001 717 9	0.666 67	0.020 408	0.039 217	0.112 427E-02	0.387 505E-02
8	0.584 86	0.467 42	0.117 44	0.002 206 9	0.799 20	0.010 101	0.038 649	0.769 710E-03	0.164 672E-02
9	0.237 17	0.168 09	0.069 08	0.000 504 5	0.708 73	0.017 857	0.041 641	0.421 593E-03	0.250 814E-02
10	0.168 09	0.115 13	0.052 96	0.000 294 6	0.684 93	0.022 222	0.046 082	0.397 488E-03	0.345 251E-02
11	**1.105 20**	**0.941 76**	**0.163 44**	**0.010 313 0**	0.852 12	0.011 628	0.062 795	**0.160 037E-02**	0.169 934E-02
12	0.559 56	0.409 86	0.149 70	0.002 239 7	0.732 47	0.013 333	0.035 218	0.955 112E-03	0.233 034E-02
13	0.207 23	0.179 60	0.027 63	0.000 508 8	**0.866 67**	0.015 773	0.092 993	***0.368 051E-03***	0.204 928E-02
14	0.267 10	0.230 26	0.036 84	0.000 714 5	0.862 07	0.013 477	0.077 691	0.483 568E-03	0.210 009E-02
15	***0.115 1***3	0.092 10	0.023 03	0.000 243 0	0.799 97	0.028 653	0.102 807	0.421 558E-03	0.457 718E-02
16	0.231 17	0.115 13	0.116 04	0.000 358 2	0.498 03	0.027 027	0.026 115	0.448 601E-03	0.389 647E-02
17	0.216 44	0.158 88	0.057 56	0.000 458 9	0.734 06	0.018 180	0.047 784	0.448 601E-03	0.282 352E-02
18	0.156 58	0.117 43	0.039 15	0.000 417 8	0.749 97	0.030 300	0.083 313	0.483 568E-03	0.411 792E-02
19	0.223 35	0.191 11	0.032 24	0.000 611 8	0.855 65	0.016 750	0.090 321	0.456 524E-03	0.238 880E-02
20	0.151 97	0.131 25	***0.020 72***	0.000 416 0	0.863 66	0.024 150	**0.132 680**	0.421 558E-03	0.321 187E-02
21	0.354 00	0.225 37	0.128 63	0.000 591 3	0.636 64	0.011 642	***0.019 991***	0.397 456E-03	0.176 357E-02

the Atlantic Ocean. The unique feature of this *in situ* experiment is that it was made in coastal waters with the largest range of variability of beam scattering coefficient known in the history of ocean optics ($0.37\,\mathrm{m}^{-1} \le b \le 9.3\,\mathrm{m}^{-1}$). The variability range of the probability of scattering was: $0.0058 \le B \le 0.0328$. The values of angular scattering coefficients have been measured at 590 scattering angles between 0.6 and 177.3 degrees. The values of these VSF for a subset of scattering angles with corresponding values of b, b_B, and B are given in Table 10.7.

10.3.5 Relationships between integral properties of experimental light scattering phase functions

Analysis of a massive database of experimental light scattering phase functions allows us to specify certain relationships between integral and angular properties of phase functions that determine their shape [81]. These parameters, presented in the decreasing order of importance, are:

$B \equiv b_B/b = 2\pi \int_{\pi/2}^{\pi} p(\lambda, \boldsymbol{x}, \cos\vartheta) \sin\vartheta \,\mathrm{d}\vartheta$ — the probability of backscattering;
$p(140^\circ)$ — the value of the phase function at 140°.
$\overline{\cos\vartheta} = 2\pi \int_0^{\pi} p(\cos\vartheta) \cos\vartheta \sin\vartheta \,\mathrm{d}\vartheta$ — the average cosine over phase function;
$\overline{\cos^2\vartheta} = 2\pi \int_0^{\pi} p(\cos\vartheta) \cos^2\vartheta \sin\vartheta \,\mathrm{d}\vartheta$ — the average square of cosine over phase function.

The probability of backscattering $B = b_B/b$ is defined by eq. (10.10). It is usually correlated with the total beam scattering coefficient [82]:

$$B = [0.5 b_W + 0.006\,18(b - b_W) + 0.003\,22(b - b_W)^2]/b, \quad r^2 = 0.88, \quad (10.20)$$

with the scattering coefficient of pure water b_W given by eq. (10.18). Relationship (10.20) is derived for typical oceanic waters, that include a total of 101 Petzold, Mankovsky and LEO-2000 measurements, it is valid for $\lambda \approx 500 \div 560\,\mathrm{nm}$ and $0.008\,\mathrm{m}^{-1} \le b \le 9.3\,\mathrm{m}^{-1}$.

The value of the phase function in the vicinity of 140° is correlated extremely well with the probability of backscattering. According to Haltrin *et al.* [82] the relationship based on more than 1000 phase functions, that include 15 Petzold [75], 41 Mankovsky [76, 77, 83], and about a thousand Lee [80] phase functions, is

$$B \equiv b_B/b = 2\pi\chi p(140^\circ), \quad b_B = 2\pi\chi\beta(140^\circ), \quad \chi = 1.15, \quad r^2 = 0.999, \quad (10.21)$$

with the phase function p normalized according to eq. (10.7). The similar relationship for scattering at angle 120° was proposed earlier by Oishi [84] and eq. (10.21) with $\chi = 1.08$ is used currently in the backscattering probe HydroScat by Hoby Labs [85].

Table 10.7a. Total angular scattering coefficients in $m^{-1}\,ster^{-1}$ measured at LEO-15 experiment in 2000 [80]

ang, $^\circ$	β_{58}	β_{59}	β_{60}	β_{57}	β_{51}	β_{16}	β_{19}
0.6	95.11	136.0	133.2	188.2	220.8	316.6	249.0
0.9	41.52	54.52	59.76	85.03	113.7	158.3	139.7
1.5	18.04	23.80	30.02	37.98	58.07	92.80	80.58
2.4	8.245	10.11	14.17	17.68	32.21	41.36	48.67
3.3	4.946	5.592	8.461	11.11	22.18	24.02	29.05
4.5	2.807	3.073	5.158	6.510	14.03	13.23	16.60
6.0	1.511	1.526	2.520	3.448	8.071	8.027	10.50
7.5	0.8835	0.8883	1.434	2.002	5.116	5.439	5.536
9.3	0.5038	0.5042	0.7735	1.048	2.931	2.796	3.120
11.4	0.2705	0.2622	0.3921	0.5267	1.517	1.594	1.727
13.5	0.1854	0.1789	0.2651	0.3763	1.042	1.150	1.162
15.6	0.1262	0.1218	0.1943	0.2550	0.7690	0.8176	0.8477
18.3	0.8264E-01	0.8177E-01	0.1287	0.1662	0.5058	0.5255	0.5498
21.0	0.6169E-01	0.6075E-01	0.9067E-01	0.1150	0.3556	0.3798	0.4029
23.7	0.4778E-01	0.4598E-01	0.6614E-01	0.8348E-01	0.2630	0.2835	0.2946
27.0	0.3321E-01	0.3248E-01	0.4682E-01	0.5951E-01	0.1849	0.1921	0.2010
30.0	0.2450E-01	0.2419E-01	0.3269E-01	0.4155E-01	0.1340	0.1447	0.1473
30.3	0.2395E-01	0.2358E-01	0.3187E-01	0.4032E-01	0.1303	0.1401	0.1440
33.6	0.1751E-01	0.1740E-01	0.2190E-01	0.2996E-01	0.9331E-01	0.1010	0.1062
37.2	0.1274E-01	0.1290E-01	0.1594E-01	0.2121E-01	0.6791E-01	0.7170E-01	0.7784E-01
41.1	0.9146E-02	0.9367E-02	0.1152E-01	0.1509E-01	0.4988E-01	0.5340E-01	0.5448E-01
45.0	0.6827E-02	0.6585E-02	0.8006E-02	0.1121E-01	0.3706E-01	0.4014E-01	0.4020E-01
49.2	0.4957E-02	0.4996E-02	0.5854E-02	0.7808E-02	0.2729E-01	0.2881E-01	0.3157E-01
53.4	0.3910E-02	0.3869E-02	0.4280E-02	0.5657E-02	0.2060E-01	0.2131E-01	0.2450E-01
57.9	0.3078E-02	0.3003E-02	0.3224E-02	0.4281E-02	0.1545E-01	0.1591E-01	0.1792E-01
63.0	0.2204E-02	0.2257E-02	0.2298E-02	0.3448E-02	0.1222E-01	0.1249E-01	0.1381E-01
67.8	0.1791E-02	0.1764E-02	0.1809E-02	0.2634E-02	0.9182E-02	0.9762E-02	0.1031E-01
72.9	0.1456E-02	0.1414E-02	0.1421E-02	0.2054E-02	0.7690E-02	0.8008E-02	0.8132E-02
78.0	0.1237E-02	0.1158E-02	0.1139E-02	0.1609E-02	0.6294E-02	0.6479E-02	0.6938E-02
83.4	0.1010E-02	0.9475E-03	0.9108E-03	0.1389E-02	0.5357E-02	0.5452E-02	0.5678E-02
90.0	0.8379E-03	0.8083E-03	0.7897E-03	0.1139E-02	0.4335E-02	0.4472E-02	0.4855E-02
95.4	0.7642E-03	0.7271E-03	0.6799E-03	0.1034E-02	0.3664E-02	0.4107E-02	0.4268E-02
101.1	0.7182E-03	0.6785E-03	0.5881E-03	0.9497E-03	0.3221E-02	0.3610E-02	0.3692E-02
107.4	0.6520E-03	0.6303E-03	0.5463E-03	0.8842E-03	0.3034E-02	0.3277E-02	0.3406E-02
113.7	0.6550E-03	0.5965E-03	0.5326E-03	0.8701E-03	0.2735E-02	0.3247E-02	0.3208E-02
120.0	0.6098E-03	0.6089E-03	0.5314E-03	0.8158E-03	0.2630E-02	0.3123E-02	0.3215E-02
127.2	0.6141E-03	0.5992E-03	0.5217E-03	0.7899E-03	0.2588E-02	0.2861E-02	0.3128E-02
127.5	0.6112E-03	0.5965E-03	0.5241E-03	0.7881E-03	0.2576E-02	0.2901E-02	0.3157E-02
134.1	0.6226E-03	0.6061E-03	0.5302E-03	0.7899E-03	0.2547E-02	0.2745E-02	0.2994E-02
148.5	0.6625E-03	0.6465E-03	0.6004E-03	0.7990E-03	0.2697E-02	0.2874E-02	0.3035E-02
140.0	0.6303E-03	0.6160E-03	0.5505E-03	0.7678E-03	0.2622E-02	0.2798E-02	0.2996E-02
156.0	0.7034E-03	0.6912E-03	0.6568E-03	0.8348E-03	0.2910E-02	0.3123E-02	0.3367E-02
163.8	0.8958E-03	0.8484E-03	0.9067E-03	0.1113E-02	0.3647E-02	0.3977E-02	0.4076E-02
172.2	0.1715E-02	0.1523E-02	0.1903E-02	0.2063E-02	0.5175E-02	0.6585E-02	0.6843E-02
177.3	0.5324E-02	0.4213E-02	0.5302E-02	0.4683E-02	0.8452E-02	0.1580E-01	0.1262E-01
b, m^{-1}	0.3796	0.4341	0.5807	0.7823	1.631	1.822	2.012
b_B, m^{-1}	0.004352	0.004059	0.003930	0.005482	0.01879	0.02025	0.02234
$B = b_B/b$	0.01147	0.009349	0.006768	0.007007	0.01152	0.01111	0.01110

Table 10.7b. Total angular scattering coefficients in $m^{-1}\,ster^{-1}$ measured at LEO-15 experiment in 2000 [80]

ang, °	β_{34}	β_{53}	β_{33}	β_{56}	β_{27}	β_{42}	β_3
0.6	565.9	358.1	531.2	413.7	677.1	638.6	643.7
0.9	254.5	181.6	235.7	210.2	335.5	320.8	309.5
1.5	107.3	98.63	108.2	117.7	185.2	157.8	158.7
2.4	47.72	50.47	53.24	63.93	76.50	69.06	83.31
3.3	25.93	32.66	30.08	44.44	43.02	39.38	40.99
4.5	13.39	19.01	16.49	26.35	21.61	19.29	22.07
6.0	6.618	11.38	10.10	13.27	11.26	10.43	12.49
7.5	4.053	6.792	6.099	8.142	6.378	6.490	7.494
9.3	2.425	4.018	3.840	4.718	3.449	4.133	4.663
11.4	1.321	2.094	2.215	2.436	1.865	2.467	2.629
13.5	0.9544	1.265	1.601	1.555	1.308	1.829	1.962
15.6	0.6978	0.9290	1.154	1.032	0.9433	1.470	1.408
18.3	0.4642	0.5862	0.7435	0.6588	0.5980	0.9914	0.9925
21.0	0.3394	0.4121	0.5374	0.4537	0.4322	0.7590	0.7704
23.7	0.2557	0.2904	0.3956	0.3249	0.3263	0.5933	0.5884
27.0	0.1835	0.1968	0.2687	0.2222	0.2232	0.4133	0.4195
30.0	0.1386	0.1426	0.1987	0.1643	0.1606	0.3186	0.3309
30.3	0.1358	0.1387	0.1933	0.1610	0.1555	0.3099	0.3226
33.6	0.1027	0.1007	0.1446	0.1185	0.1150	0.2329	0.2499
37.2	0.7581E-01	0.7499E-01	0.1062	0.8664E-01	0.8427E-01	0.1796	0.1935
41.1	0.5751E-01	0.5598E-01	0.7839E-01	0.6306E-01	0.6481E-01	0.1365	0.1468
45.0	0.4423E-01	0.4286E-01	0.5865E-01	0.4653E-01	0.4794E-01	0.1062	0.1145
49.2	0.3402E-01	0.3013E-01	0.4308E-01	0.3410E-01	0.3433E-01	0.8208E-01	0.9010E-01
53.4	0.2623E-01	0.2323E-01	0.3260E-01	0.2569E-01	0.2568E-01	0.6520E-01	0.7026E-01
57.9	0.1994E-01	0.1778E-01	0.2451E-01	0.1922E-01	0.2012E-01	0.5096E-01	0.5659E-01
63.0	0.1509E-01	0.1318E-01	0.1920E-01	0.1475E-01	0.1458E-01	0.3911E-01	0.4273E-01
67.8	0.1215E-01	0.1040E-01	0.1501E-01	0.1134E-01	0.1163E-01	0.3071E-01	0.3465E-01
72.9	0.1009E-01	0.8223E-02	0.1192E-01	0.8969E-02	0.9113E-02	0.2479E-01	0.2791E-01
78.0	0.8313E-02	0.6715E-02	0.1010E-01	0.7307E-02	0.7123E-02	0.2033E-01	0.2370E-01
83.4	0.6962E-02	0.5445E-02	0.8134E-02	0.5858E-02	0.6091E-02	0.1668E-01	0.1949E-01
90.0	0.5926E-02	0.4345E-02	0.6596E-02	0.4696E-02	0.4816E-02	0.1368E-01	0.1647E-01
95.4	0.5126E-02	0.3855E-02	0.5852E-02	0.4053E-02	0.4204E-02	0.1203E-01	0.1482E-01
101.1	0.4696E-02	0.3468E-02	0.5167E-02	0.3604E-02	0.3554E-02	0.1092E-01	0.1320E-01
107.4	0.4323E-02	0.3090E-02	0.4606E-02	0.3249E-02	0.3489E-02	0.9711E-02	0.1238E-01
113.7	0.3997E-02	0.3105E-02	0.4398E-02	0.3131E-02	0.3196E-02	0.9359E-02	0.1169E-01
120.0	0.3808E-02	0.2729E-02	0.4039E-02	0.3004E-02	0.3039E-02	0.8897E-02	0.1098E-01
127.2	0.3765E-02	0.2723E-02	0.3920E-02	0.2984E-02	0.3074E-02	0.8735E-02	0.1056E-01
127.5	0.3773E-02	0.2742E-02	0.3911E-02	0.2916E-02	0.3109E-02	0.8755E-02	0.1054E-01
134.1	0.3679E-02	0.2686E-02	0.4039E-02	0.2943E-02	0.2997E-02	0.8775E-02	0.1061E-01
148.5	0.3906E-02	0.2938E-02	0.4162E-02	0.3117E-02	0.3109E-02	0.9252E-02	0.1081E-01
140.0	0.3722E-02	0.2825E-02	0.4108E-02	0.2925E-02	0.3027E-02	0.8863E-02	0.1059E-01
156.0	0.3988E-02	0.3133E-02	0.4338E-02	0.3402E-02	0.3324E-02	0.9644E-02	0.1098E-01
163.8	0.4642E-02	0.4131E-02	0.5239E-02	0.4653E-02	0.4006E-02	0.1080E-01	0.1204E-01
172.2	0.6291E-02	0.7727E-02	0.7133E-02	0.9094E-02	0.6319E-02	0.1391E-01	0.1454E-01
177.3	0.8684E-02	0.1503E-01	0.1080E-01	0.1814E-01	0.1137E-01	0.2204E-01	0.1598E-01
b, m^{-1}	2.102	2.256	2.495	2.739	3.009	3.296	3.533
b_B, m^{-1}	0.02657	0.02020	0.02869	0.02078	0.02167	0.06251	0.07637
$B = b_B/b$	0.01264	0.008952	0.01150	0.007587	0.007203	0.01896	0.02162

Table 10.7c. Total angular scattering coefficients in $m^{-1}\,ster^{-1}$ measured at LEO-15 experiment in 2000 [80]

ang, $^\circ$	β_{37}	β_4	β_{47}	β_{46}	β_{45}	β_{41}	β_{48}
0.6	688.0	802.8	899.9	966.8	952.4	815.5	107.1
0.9	373.8	389.6	440.7	506.2	512.7	421.1	588.6
1.5	213.1	183.5	188.4	200.1	208.9	219.5	310.3
2.4	104.9	79.92	83.40	91.90	85.87	100.3	155.2
3.3	61.04	40.89	43.17	45.01	53.07	60.45	93.51
4.5	31.59	21.91	23.18	23.51	24.54	32.99	54.30
6.0	15.54	12.04	12.06	12.77	13.06	17.92	29.91
7.5	9.049	7.774	7.856	8.557	8.069	11.39	19.45
9.3	5.053	4.804	5.072	5.424	5.246	7.201	12.56
11.4	2.544	2.683	3.070	3.179	3.168	4.309	7.868
13.5	1.635	2.045	2.340	2.428	2.437	3.261	6.121
15.6	1.137	1.526	1.771	1.834	1.819	2.451	4.763
18.3	0.7221	1.046	1.286	1.310	1.330	1.752	3.498
21.0	0.4984	0.8140	1.024	1.060	1.064	1.382	2.811
23.7	0.3553	0.6377	0.8057	0.8362	0.8548	1.085	2.207
27.0	0.2441	0.4652	0.5918	0.6185	0.6192	0.7824	1.625
30.0	0.1748	0.3553	0.4669	0.4823	0.4930	0.6158	1.273
30.3	0.1704	0.3449	0.4583	0.4681	0.4829	0.6004	1.244
33.6	0.1226	0.2622	0.3583	0.3692	0.3809	0.4639	0.9657
37.2	0.8822E-01	0.2073	0.2839	0.2926	0.3019	0.3593	0.7531
41.1	0.6377E-01	0.1584	0.2250	0.2384	0.2437	0.2776	0.5927
45.0	0.4694E-01	0.1264	0.1833	0.1894	0.1931	0.2195	0.4719
49.2	0.3424E-01	0.9764E-01	0.1446	0.1543	0.1538	0.1724	0.3697
53.4	0.2562E-01	0.7738E-01	0.1189	0.1234	0.1282	0.1385	0.2977
57.9	0.1917E-01	0.6118E-01	0.9754E-01	0.1012	0.1049	0.1108	0.2403
63.0	0.1405E-01	0.4793E-01	0.7712E-01	0.8041E-01	0.8182E-01	0.8559E-01	0.1866
67.8	0.1124E-01	0.3860E-01	0.6341E-01	0.6597E-01	0.6727E-01	0.6861E-01	0.1516
72.9	0.9007E-02	0.3088E-01	0.5202E-01	0.5474E-01	0.5519E-01	0.5552E-01	0.1216
78.0	0.7355E-02	0.2616E-01	0.4277E-01	0.4491E-01	0.4601E-01	0.4523E-01	0.9927E-01
83.4	0.6118E-02	0.2176E-01	0.3583E-01	0.3761E-01	0.3880E-01	0.3779E-01	0.8257E-01
90.0	0.4927E-02	0.1810E-01	0.2973E-01	0.3143E-01	0.3212E-01	0.3122E-01	0.6727E-01
95.4	0.4291E-02	0.1620E-01	0.2625E-01	0.2763E-01	0.2804E-01	0.2732E-01	0.5913E-01
101.1	0.3851E-02	0.1471E-01	0.2334E-01	0.2462E-01	0.2534E-01	0.2480E-01	0.5331E-01
107.4	0.3448E-02	0.1342E-01	0.2129E-01	0.2240E-01	0.2285E-01	0.2220E-01	0.4796E-01
113.7	0.3152E-02	0.1284E-01	0.2005E-01	0.2067E-01	0.2118E-01	0.2106E-01	0.4548E-01
120.0	0.3066E-02	0.1238E-01	0.1906E-01	0.2039E-01	0.2022E-01	0.2020E-01	0.4324E-01
127.2	0.2976E-02	0.1193E-01	0.1863E-01	0.1920E-01	0.1967E-01	0.1979E-01	0.4215E-01
127.5	0.2983E-02	0.1193E-01	0.1859E-01	0.1916E-01	0.1958E-01	0.1974E-01	0.4215E-01
134.1	0.2948E-02	0.1158E-01	0.1829E-01	0.1956E-01	0.1958E-01	0.1988E-01	0.4196E-01
148.5	0.3116E-02	0.1190E-01	0.1876E-01	0.1969E-01	0.2036E-01	0.2039E-01	0.4294E-01
140.0	0.2989E-02	0.1165E-01	0.1833E-01	0.1902E-01	0.1954E-01	0.1997E-01	0.4209E-01
156.0	0.3354E-02	0.1224E-01	0.1911E-01	0.1997E-01	0.2055E-01	0.2096E-01	0.4374E-01
163.8	0.4194E-02	0.1323E-01	0.2043E-01	0.2100E-01	0.2157E-01	0.2231E-01	0.4333E-01
172.2	0.7089E-02	0.1595E-01	0.2313E-01	0.2428E-01	0.2420E-01	0.2418E-01	0.3714E-01
177.3	0.8822E-02	0.1856E-01	0.3517E-01	0.3920E-01	0.3646E-01	0.3771E-01	0.4496E-01
b, m^{-1}	3.720	3.797	4.386	4.650	4.668	5.367	9.263
b_B, m^{-1}	0.02164	0.08509	0.1330	0.1400	0.1435	0.1420	0.3034
$B = b_B/b$	0.005818	0.02241	0.03032	0.03011	0.03074	0.02646	0.03276

The best relationship between average cosine and probability of backscattering is given by Haltrin [86]:

$$\overline{\cos(\vartheta)} = 2\frac{1-2B}{2+B}, \quad r^2 = 0.999, \tag{10.22}$$

This relationship is derived from experimental data by Timofeyeva [87–89], corrected to match theoretical asymptotics for isotropic ($B = 0.5$, $\overline{\cos(\vartheta)} = 0$) and delta-shaped scattering ($B = 0$, $\overline{\cos(\vartheta)} = 1$), and later successfully tested with the available database of more than 1000 experimental phase functions.

The second physically correct relationship derived by Haltrin [86] from Timofeyeva's [87–89] data,

$$\overline{\cos^2(\vartheta)} = \frac{6-7B}{3(2+B)}, \quad r^2 = 0.999, \tag{10.23}$$

did not pass as well as eq. (10.21) the applicability test on a set of newly measured phase functions. Instead, some alternative regionally dependent 'non-physical' regressional relationship

$$\overline{\cos^2(\vartheta)} = 0.985\,\overline{\cos(\vartheta)}, \quad r^2 = 0.996, \tag{10.24}$$

was proposed [80].

10.4 Raman scattering of light in natural water

The model of Raman scattering is presented here according to Haltrin and Kattawar [30] with corrections by Gordon [28], Faris and Copeland [27], and Bartlett *et al.* [23]. The frequency redistribution is derived from the works by Walrafen [42, 43]. To be consistent with the elastic scattering and absorption models the Raman scattering model is presented in a wavelength representation.

The wavelength distribution of the Raman scattering coefficient is:

$$\sigma^R(\lambda', \lambda, \cos\vartheta) = b^R(\lambda', \lambda) f^R(\lambda', \lambda) p_R(\lambda', \lambda, \cos\vartheta), \tag{10.25}$$

$$\left.\begin{aligned} b^R(\lambda', \lambda) &= b_0^R \frac{v^4}{(v_i^2 - v'^2)^2} \equiv b_0^R \left[\frac{\lambda_i^2 \lambda'^2}{\lambda^2(\lambda'^2 - \lambda_i^2)}\right]^2, \\ b_0^R &= 0.018\,\mathrm{m}^{-1}, \quad v_i = 88.000\,\mathrm{cm}^{-1}, \quad \lambda_i \simeq 113.636\,\mathrm{nm}, \end{aligned}\right\} \tag{10.26}$$

here $b^R(\lambda', \lambda)$ is a total Raman scattering coefficient, λ' and λ (in nanometers) are wavelengths of excitation and emission, $\nu' = k_\nu/\lambda'$, and $\nu = k_\nu/\lambda$ are excitation and emission wave numbers (both in inverse centimeters), $k_\nu = 1 \equiv 10^7\,\mathrm{nm/cm}$, ν_i and λ_i are frequency and wavelength of intermediate resonance [27], p_R is a Raman angular scattering phase function [28, 90]:

$$p_R(\lambda', \lambda, \cos\vartheta) = \frac{3}{4\pi[3 + \gamma(\nu_S)]}[1 + \gamma(\nu_S)\cos^2\vartheta], \tag{10.27}$$

$$\gamma(\nu_S) = \frac{1-\rho(\nu_S)}{1+3\rho(\nu_S)}, \quad \nu_S = \nu' - \nu \equiv \frac{k_\nu(\lambda-\lambda')}{\lambda\lambda'} \tag{10.27a}$$

p_R is normalized according to eq. (10.7), $\rho(\nu_S)$ is the Raman depolarization ratio, and

$$f^R(\lambda',\lambda) = -\frac{\mathrm{d}\nu'}{\mathrm{d}\lambda'}\sigma^R_\nu(\nu',\nu) = \frac{\nu'^2}{k_\nu} f^R_\nu(\nu',\nu), \tag{10.28}$$

$$\int f^R_\nu(\nu',\nu)\,\mathrm{d}\nu' \equiv \int f^R_\nu(\nu',\nu)\,\mathrm{d}\nu \equiv \int f^R_\nu(\nu_S)\,\mathrm{d}\nu_S = 1, \tag{10.28a}$$

is the frequency redistribution of Raman-scattered light. The Raman depolarization ratio $\rho(\nu_S)$ is given in Table 10.8 and shown with $\gamma(\nu_S)$ in Fig. 10.2.

The Raman scattering frequency redistribution is represented according to the data of Walrafen [42, 43], namely:

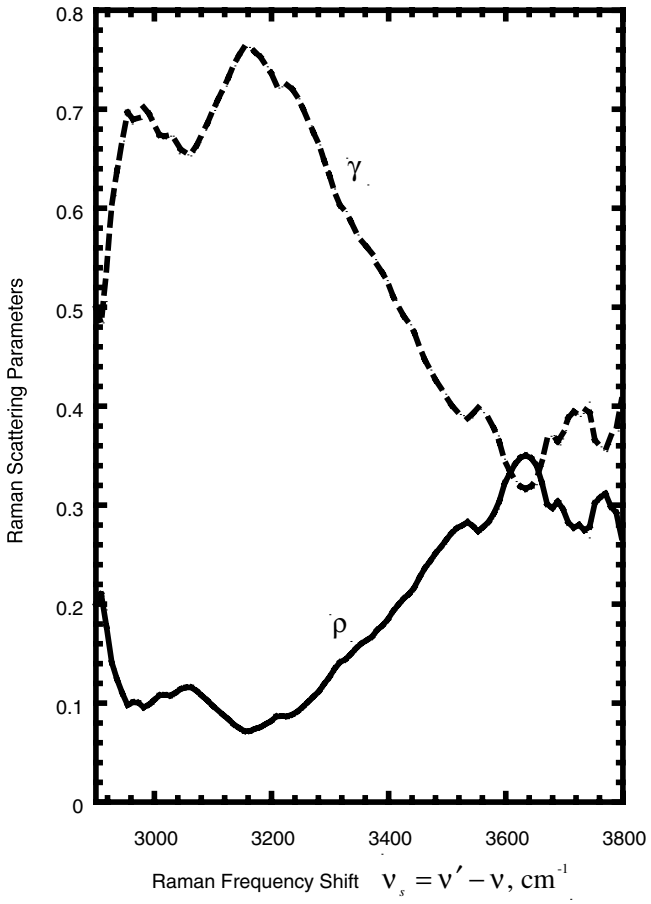

Fig. 10.2. Raman scattering parameters as a function of frequency shift

Table 10.8. Raman depolarization ratio $\rho(\nu_S)$ and parameter $\gamma(\nu_S)$; ν_S in cm^{-1}

ν_S	ρ	γ	ν_S	ρ	γ	ν_S	ρ	γ	ν_S	ρ	γ
2900.0	0.20052	0.49919	3125.8	0.084249	0.73099	3350.7	0.15928	0.56888	3575.8	0.28748	0.38257
2905.2	0.20846	0.48699	3130.1	0.081258	0.73867	3355.0	0.16076	0.56618	3580.1	0.29194	0.37747
2910.4	0.20945	0.48549	3135.3	0.078762	0.74517	3360.2	0.16274	0.56259	3585.4	0.29740	0.37131
2915.5	0.19552	0.50706	3140.4	0.076763	0.75042	3365.4	0.16471	0.55905	3590.6	0.30732	0.36040
2920.6	0.16073	0.56624	3145.6	0.074764	0.75573	3370.6	0.16669	0.55551	3595.8	0.31924	0.34773
2925.7	0.14382	0.59812	3150.8	0.072268	0.76243	3375.8	0.17016	0.54939	3600.2	0.32469	0.34209
2930.8	0.13586	0.61392	3155.1	0.071762	0.76380	3380.1	0.17363	0.54335	3605.4	0.33064	0.33604
2935.1	0.12641	0.63339	3160.3	0.071750	0.76383	3385.3	0.17660	0.53824	3610.6	0.33610	0.33058
2940.2	0.11745	0.65260	3165.5	0.072236	0.76252	3390.5	0.17907	0.53404	3615.8	0.34155	0.32522
2945.4	0.10999	0.66920	3170.7	0.073715	0.75854	3395.7	0.18253	0.52822	3620.1	0.34452	0.32233
2950.5	0.099046	0.69457	3175.9	0.075194	0.75459	3400.0	0.18551	0.52327	3625.3	0.34799	0.31899
2955.7	0.098538	0.69578	3180.2	0.075682	0.75329	3405.2	0.19146	0.51356	3630.5	0.35245	0.31475
2960.0	0.10250	0.68642	3185.4	0.076664	0.75068	3410.4	0.19492	0.50801	3635.7	0.34946	0.31759
2965.2	0.10050	0.69113	3190.6	0.079137	0.74419	3415.6	0.19889	0.50174	3640.8	0.34597	0.32093
2970.4	0.10049	0.69115	3195.7	0.081610	0.73776	3420.8	0.20236	0.49633	3645.2	0.34844	0.31856
2975.6	0.10048	0.69117	3200.1	0.082097	0.73651	3425.2	0.20533	0.49175	3650.3	0.34495	0.32192
2980.7	0.095998	0.70187	3205.3	0.085067	0.72891	3430.4	0.20830	0.48723	3655.5	0.33351	0.33316
2985.1	0.096485	0.70070	3210.5	0.087540	0.72267	3435.6	0.21077	0.48350	3660.6	0.32605	0.34070
2990.3	0.098461	0.69596	3215.6	0.087032	0.72395	3440.8	0.21374	0.47907	3665.7	0.30964	0.35790
2995.4	0.099941	0.69245	3220.8	0.086524	0.72523	3445.1	0.21820	0.47250	3670.0	0.30218	0.36601
3000.6	0.10390	0.68316	3225.1	0.086514	0.72525	3450.3	0.22465	0.46319	3675.2	0.29769	0.37099
3005.8	0.10787	0.67401	3230.3	0.087496	0.72278	3455.5	0.22961	0.45617	3680.4	0.29719	0.37155
3010.2	0.10786	0.67404	3235.5	0.088479	0.72032	3460.7	0.23506	0.44860	3685.6	0.30016	0.36824
3015.3	0.10834	0.67294	3240.7	0.089958	0.71664	3465.0	0.23903	0.44317	3690.8	0.30561	0.36226
3020.5	0.10833	0.67296	3245.0	0.091936	0.71176	3470.2	0.24299	0.43784	3695.1	0.30013	0.36828
3025.7	0.10782	0.67413	3250.2	0.094409	0.70571	3475.4	0.24745	0.43192	3700.2	0.29267	0.37664
3030.0	0.10781	0.67415	3255.4	0.097379	0.69855	3480.6	0.25191	0.42608	3705.4	0.28471	0.38578
3035.2	0.10979	0.66965	3260.6	0.10035	0.69148	3485.8	0.25637	0.42034	3710.5	0.27824	0.39339
3040.4	0.11574	0.65636	3265.8	0.10332	0.68451	3490.2	0.25835	0.41782	3715.7	0.27723	0.39459
3045.6	0.11424	0.65968	3270.1	0.10579	0.67878	3495.4	0.26182	0.41344	3720.0	0.27822	0.39341
3050.8	0.11473	0.65859	3275.3	0.10876	0.67198	3500.6	0.26727	0.40666	3725.2	0.28019	0.39108
3055.1	0.11621	0.65532	3280.5	0.11173	0.66528	3505.8	0.27074	0.40241	3730.4	0.27770	0.39403
3060.3	0.11669	0.65427	3285.7	0.11570	0.65645	3510.1	0.27321	0.39942	3735.5	0.27371	0.39881
3065.5	0.11519	0.65757	3290.1	0.11966	0.64779	3515.3	0.27618	0.39585	3740.7	0.26823	0.40548
3070.6	0.11319	0.66201	3295.3	0.12363	0.63927	3520.5	0.27866	0.39289	3745.1	0.28512	0.38531
3075.8	0.11069	0.66762	3300.5	0.12759	0.63091	3525.7	0.27964	0.39173	3750.3	0.30101	0.36730
3080.1	0.10820	0.67326	3305.7	0.13255	0.62065	3530.0	0.28062	0.39057	3755.5	0.30398	0.36404
3085.3	0.10521	0.68012	3310.9	0.13800	0.60962	3535.2	0.28310	0.38766	3760.7	0.30744	0.36027
3090.5	0.10271	0.68593	3315.2	0.14048	0.60468	3540.4	0.28159	0.38943	3765.1	0.31041	0.35707
3095.6	0.099222	0.69415	3320.4	0.14245	0.60080	3545.5	0.27761	0.39414	3770.3	0.31189	0.35549
3100.8	0.096727	0.70011	3325.6	0.14393	0.59790	3550.7	0.27412	0.39832	3775.4	0.30542	0.36247
3105.1	0.094729	0.70494	3330.8	0.14690	0.59214	3555.0	0.27411	0.39833	3780.6	0.29696	0.37181
3110.3	0.091737	0.71225	3335.1	0.14938	0.58739	3560.2	0.27708	0.39477	3785.7	0.29049	0.37912
3115.5	0.089241	0.71842	3340.3	0.15235	0.58176	3565.4	0.28055	0.39066	3790.0	0.29297	0.37630
3120.6	0.086745	0.72467	3345.5	0.15631	0.57436	3570.6	0.28302	0.38775	3797.7	0.26761	0.40624

$$f_\nu^R(\nu',\nu) = k^R \sum_{i=1}^{4} \alpha_i \exp\left[-\frac{(\nu'-\nu-\Delta\nu_i)^2}{2\sigma_i^2}\right],$$
$$f_\nu^R(\nu_S) = k^R \sum_{i=1}^{4} \alpha_i \exp\left[-\frac{(\nu_S-\Delta\nu_i)^2}{2\sigma_i^2}\right], \tag{10.29}$$

where

$$k^R = \left(\sqrt{2\pi}\sum_{i=1}^{4}\alpha_i\sigma_i\right)^{-1} = 5.152\cdot 10^{-3}\,\text{cm}.$$

Values of α_i, $\Delta\nu_i$, and σ_i are given in Table 10.9. The Raman scattering model presented here coincides with the Haltrin and Kattawar [30] model if we neglect $\nu^2 \simeq 4\times 10^8\,\text{cm}^{-2}$ in eq. (10.26) in comparison with $\nu_i^2 \approx 7.7\times 10^9\,\text{cm}^{-2}$ and set γ in eq. (10.27) to be equal to 0.6.

Table 10.9. Raman frequency distribution parameters [30]

i	α_i	$\Delta\nu_i$, cm^{-1}	σ_i, cm^{-1}
1	0.41	3250	89.179
2	0.39	3425	74.317
3	0.10	3530	59.453
4	0.10	3625	59.453

10.5 Chlorophyll fluorescence in natural water

The chlorophyll or red fluorescence is represented according to Gordon [48] in the interpretation of Haltrin and Kattawar [30]:

$$\sigma^C(\lambda',\lambda,\cos\gamma) \equiv \sigma^C(\lambda',\lambda) = a_C^0(\lambda')C_C\eta^C(\lambda',\lambda), \tag{10.30}$$

$$\eta^C(\lambda',\lambda) = \begin{cases} \dfrac{\eta_0^C}{4\pi}\dfrac{\lambda'}{\lambda_{0F}}\dfrac{1}{\sqrt{2\pi\sigma^2}}\exp\left[-\dfrac{(\lambda-\lambda_{0F})^2}{2\sigma^2}\right], & 370\,\text{nm}\le\lambda'\le 690\,\text{nm} \\ 0, & \text{elsewhere,} \end{cases} \tag{10.31}$$

here $\eta_0^C \simeq 0.05$ (an average value by Kiefer [51]), $\lambda_{0F} \simeq 683\,\text{nm}$, $\sigma = 10.6\,\text{nm}$.

10.6 Yellow substance (Gelbstoff, DOM or CDOM) fluorescence in natural water

The most advanced yellow substance fluorescence model was proposed by Hawes *et al.* [49]. According to this model, the yellow substance components fluorescence emission coefficient can be expressed as follows:

$$\chi^j(\lambda',\lambda) = a_j(\lambda')\eta^j(\lambda',\lambda) \equiv a_j^0\exp(-k_j\lambda')\eta^j(\lambda',\lambda), \quad j=F,H, \tag{10.32}$$

with the coefficients a_j^0 and k_j given in Table 10.2, and the spectral fluorescence efficiency function η^j represented by the following empirical equation:

$$\eta^j(\lambda', \lambda) = A_0^j(\lambda') \exp\left\{ - \left[\frac{1/\lambda - A_1^j/\lambda' - B_1^j}{0.6(A_2^j/\lambda' + B_2^j)} \right]^2 \right\}, \quad j = F, H, \qquad (10.33)$$

with the coefficients $A_0^j(\lambda')$, A_1^j, A_2^j, B_1^j, B_2^j given in Table 10.10a and 10.10b. This model is more advanced than the model for chlorophyll fluorescence because the predominant part of yellow substance or DOM is dissolved in water and the yellow substance is easier to process experimentally than the chlorophyll which is imbedded into living phytoplanktonic cells [1].

Table 10.10a. Parameters for fluorescence model $\eta(\lambda_x, \lambda_m)$ of fulvic and humic acids [49]

	λ_x, nm	Fulvic acid				Humic acid				
		FA7	FA8	FA9	FA11	HA1	HA2	HA4	HA6	HA8
$A_0(\lambda_x)$	310	5.18	4.48	5.21	5.09	2.49	2.78	4.83	5.77	3.61
$\times 10^5$	330	6.34	5.67	6.57	6.27	2.68	3.13	5.11	6.86	4.01
	350	8.00	7.23	7.93	7.93	2.95	3.73	5.94	7.27	0.46
	370	9.89	9.26	9.93	9.76	3.34	4.42	7.20	8.37	5.48
	390	9.39	9.06	**9.93**	8.72	2.77	4.03	6.53	7.08	5.06
	410	10.48	9.22	9.47	7.93	2.26	3.91	6.41	7.80	5.05
	430	12.59	10.14	10.21	8.15	2.63	4.41	7.66	8.90	5.66
	450	13.48	9.90	10.08	7.75	2.72	4.52	7.55	9.30	5.70
	470	13.61	9.70	10.11	7.70	2.65	4.75	7.88	8.41	5.32
	490	9.27	7.90	8.34	5.98	2.20	4.29	6.81	6.68	4.42
A_1		0.470	0.389	0.466	0.471	0.304	0.379	0.346	0.447	0.356
$B_1 \times 10^4$		8.077	10.073	8.340	8.204	12.169	10.043	10.891	8.594	10.694
A_2		0.407	0.386	0.386	0.386	0.591	0.362	0.411	0.417	0.406
$B_2 \times 10^4$		−4.57	−4.20	−4.13	−4.20	−9.39	−3.17	−4.60	−4.64	−4.42
r^2		0.987	0.989	0.975	0.991	0.712	0.985	0.985	0.985	0.986

Table 10.10b. FA and HA fluorescence sample information [49]

Sample name	Location	Sample date	Sample volume, liters	Extraction Method	Total Mass extracted (mg)
HA1	Peru upwelling (El Niño)	—	—	XAD2	—
HA2	Gulf of Mexico, outside Loop Cur.	—	—	XAD2	—
HA4	Gulf of Mexico, mouth of Tampa Bay	12 October 1989	26	XAD2	0.156
HA6	Gulf of Mexico, mid-West Florida shelf	4 March, 1990	55	XAD2	0.65
FA7	Gulf of Mexico, mid-West Florida shelf	4 March, 1990	32	C18	12.66
FA8, HA8	Gulf of Mexico, mouth of Tampa Bay	5 March, 1990	20	C18	2.24, 0.42
FA9	North Atlantic, 60°N 20°W	24 May 1991	55	C18	19.06
FA11	North Atlantic, 60°N 20°W	20 August 1991	55	C18	6.99

10.7 Diffuse reflection coefficient

The diffuse reflection coefficient (DRC), or diffuse reflectance (DR), or albedo of the sea just below the sea surface, is defined as a ratio of upward to downward irradiance at the level just below the sea surface. It is a very important apparent optical property and constituent part of the remote sensing coefficient [91, 92] that is used to extract information from remotely measured optical images of the ocean. As an apparent optical property it depends not only on inherent optical properties but also on conditions of illumination just below the sea surface. The theory and experiments show that DRC depends only on two inherent optical properties, the absorption coefficient, a, and the backscattering coefficient, b_B, that is derived from the angular scattering coefficient. Dependence on other properties (or moments) of angular scattering coefficient is weak and can be neglected. The diffuse reflection coefficient of open ocean illuminated by diffuse light can be written in a very simple way:

$$R = k\frac{b_B}{a}, \quad R = k\frac{b_B}{a + b_B}. \tag{10.34}$$

The second variant in eqs (10.34) is preferable because it does not give infinite values for R at $a = 0$. According to Morel and Prieur [93] for open ocean water $k = 1/3$. Equations (10.34) are widely used to describe DRC of the ocean. The

big shortcoming of eqs (10.34) is that they do not satisfy physical conditions that restrict values of diffuse reflection coefficient:

$$0 \le R \le 1. \tag{10.35}$$

At zero backscattering $b_B = 0$ the DRC should be equal to zero (no light returns from the water depth), and at zero absorption $a = 0$ DRC should by equal to 1 (all light is eventually reflected back). Both eqs (10.34) only satisfy the first condition, but do not satisfy the second one. At zero absorption value the first equation gives infinity, and the second one gives $k < 1$. This means that eqs (10.34) are only rough approximations. The theoretical analysis shows that they are good only for rather small values of Gordon's parameter:

$$x_G = \frac{b_B}{a + b_B} < 0.1, \quad \text{or} \quad a > 9b_B. \tag{10.36}$$

In addition to theoretical considerations there is experimental data by Timofeyeva [107] who measured the DRC in a wide range of Gordon's parameter (see Table 10.11). The measurements have been made in marine waters for smaller values of x_G and in artificially created absorbing and scattering substances for higher values of x_G. These data together with the DRC computed with different equations are shown in Fig. 10.3. Some authors try to improve eqs (10.34) by representing DRC with a series over b_B/a or x_G, but this method is useless for $x_G > 0.9$. According to Gate [95], asymptotics of the DRC for x_G close to one described by the following equation:

$$R = \frac{\sqrt{6x_G} - 2\sqrt{1 - x_G}}{\sqrt{6x_G} + 2\sqrt{1 - x_G}} \equiv \frac{1 - \sqrt{2a/(3b_B)}}{1 + \sqrt{2a/(3b_B)}} \equiv \frac{\sqrt{3b_B/(2a)} - 1}{\sqrt{3b_B/(2a)} + 1}, \quad 1 - x_G < 0.1. \tag{10.37}$$

It is clear that this dependence could not be described by any power series for small x_G or small ratios b_B/a.

Table 10.11. Downward and upward average cosines and diffuse reflectance as a function of average cosine over radiance distribution according to *in situ* and modeling experiments by V. A. Timofeyeva [107]

$\overline{\mu}$	$\overline{\mu}_d$	$\overline{\mu}_u$	R_∞
0.1	0.5249	0.4831	0.671
0.2	0.5525	0.4545	0.443
0.3	0.5834	0.4202	0.283
0.4	0.6184	0.3745	0.171
0.5	0.6566	0.3311	0.095
0.6	0.7008	0.3003	0.048
0.7	0.7536	0.2857	0.0207
0.8	0.8217	0.3610	0.0082
0.9	0.9033	0.6849	0.0016

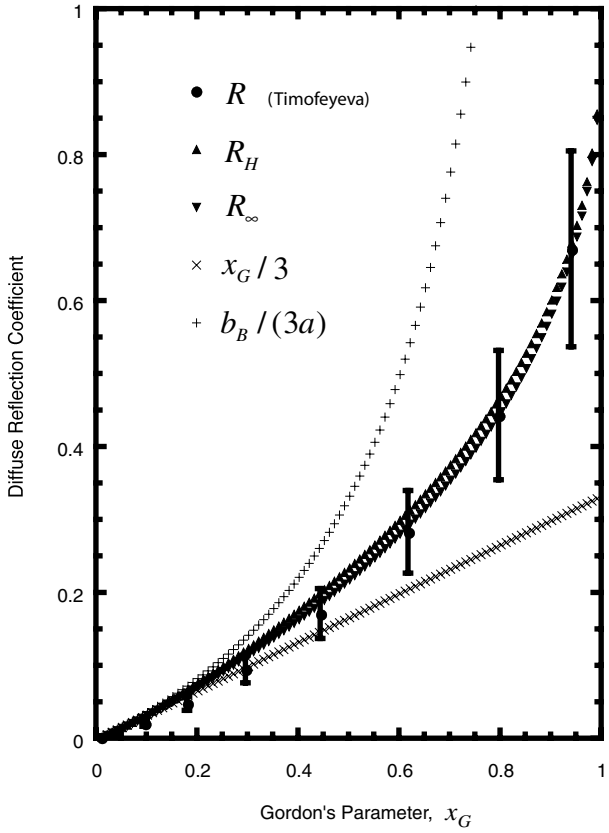

Fig. 10.3. Diffuse reflection coefficient of natural water basin according to experiment, and to linear, and nonlinear theories

Fortunately, there are several equations available in the literature that satisfy physical condition (10.35) and give good approximation to the DRC of the seawater basin with arbitrary values of optical properties.

The first such equation was proposed by Haltrin [96]:

$$R = \frac{1-\overline{\mu}_H}{1+\overline{\mu}_H}\left(\sqrt{1+\overline{\mu}_H^2}-\overline{\mu}_H\right)^2, \tag{10.38}$$

$$\overline{\mu}_H = \sqrt{\frac{a}{a+(4+2\sqrt{2})b_B}} \equiv \sqrt{\frac{1-x_G}{1+(3+2\sqrt{2})x_G}}. \tag{10.39}$$

It was derived as a result of the exact solution of the radiative transfer equation in the asymptotic regime ($cz \gg 1$, where z is a physical depth in m^{-1}) with the phase function approximated as:

$$p_H(\cos\vartheta) = \frac{1}{4\pi}\left[2g\delta(1-\cos\vartheta)+\frac{1-g}{\sqrt{2(1-\cos\vartheta)}}\right], \tag{10.40}$$

here δ is a Dirac's delta function, and $g = 1 - (2 + \sqrt{2})B$ is an average cosine over phase function p_H, with $B = b_B/b$ being a probability of backscattering (see eq. (10.10)).

The exact solution of the RTE in the asymptotic regime with the phase function (40) is given by the following equation:

$$L_\infty(z,\theta) = \frac{L_0(1-\overline{\mu}_H^2)\exp(-az/\overline{\mu}_H)}{(1+\overline{\mu}_H^2 - 2\overline{\mu}_H\cos\theta)^{3/2}}, \tag{10.41}$$

where L_0 is determined by the boundary conditions, and $\overline{\mu}_H$ is given by eq. (10.39). The shape of radiance distribution (10.41) is a Henyey–Greenstein function [97].

Another analytic equation was proposed in the framework of the self-consistent approximation to the RTE [98, 99]:

$$R = R_\infty = \left(\frac{1-\overline{\mu}}{1+\overline{\mu}}\right)^2, \tag{10.42}$$

with the average cosine $\overline{\mu}$ over radiance distribution in the asymptotic regime given by

$$\overline{\mu} = \sqrt{\frac{a}{a+3b_B+\sqrt{b_B(4a+9b_B)}}} \equiv \sqrt{\frac{1-x_G}{1+2x_G+\sqrt{x_G(4+5x_G)}}}. \tag{10.43}$$

Equations (10.42) and (10.43) give almost the same values for R as eqs (10.38) and (10.39) (see Fig. 10.3), but they can be generalized to the cases of finite water depth and combined illumination of water surface by the light of the sun and the sky.

Equations (10.42) and (10.43) and (10.38) and (10.39) seem more complex than simple linear eqs (10.34). But they are good for any value of Gordon's parameter x_G (or for any arbitrary pair of values a and b_B: $0 \le a \le \infty$, $0 \le b_B \le \infty$), and satisfy all physical conditions outline above, while eqs (10.34) fail for values of $x_G > 0.1$. The question arises, is it worth to use more complex expressions instead of the very simple linear expressions (10.34)? The answer can be obtained from the analysis of frequency distribution of Gordon's parameter values in natural waters. Extensive *in situ* measurements show that in the following three cases: (a) waters of the open ocean, (b) clear inland water basins, like Lake Baikal, and (c) biologically stable waters of marine coastal areas and certain lakes Gordon's coefficient $x_G < 0.1$ and simple linear equations (10.34) can be used without inflicting unacceptable error. At the same time certain inland waters, coastal ocean waters, and even whole seas contain large number of scattering particles such as detritus with low absorption which results in much higher values of Gordon's parameter. Fig. 10.4 shows a frequency distribution (histogram) of Gordon's parameter in the Yellow Sea [100]. It shows that about 50% of all values of x_G exceed the critical value of 0.1 and some values of this parameter are as large as 0.9. It means that for the Yellow Sea water types we should use the nonlinear equations given above.

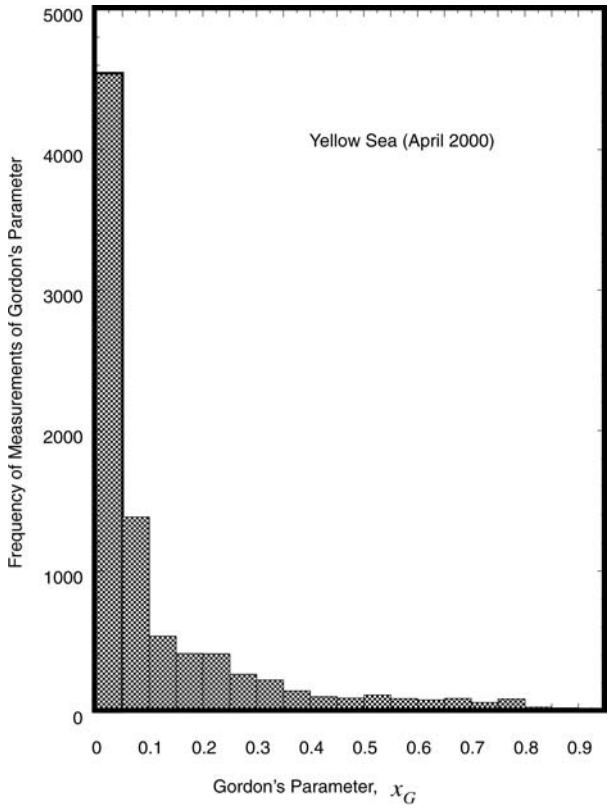

Fig. 10.4. Frequency distribution of measured Gordon's parameter in waters of Yellow Sea

Another reason to use the nonlinear approach is that it can be generalized to the case of shallow water depth and to the case that takes into account the combined illumination of water surface by the direct light of the sun and the diffuse light of the sky.

10.8 Diffuse reflection coefficient of a water basin illuminated by direct solar light and diffuse light of the sky

The diffuse reflection coefficient of water illuminated by the light of the sun and the sky was considered by several authors. Here we restrict ourselves to the solution that is valid for all optical water types and validated with experimental data [101].

The DRC of the water body illuminated by the light of the sun and the sky is a linear combination of DRC for diffuse illumination R_∞ and the DRC

for directed illumination R_s with the weight determined by the ratio of direct irradiance to the diffuse irradiance just below the water surface, q_w:

$$R = \frac{R_\infty + q_w R_s}{1 + q_w}, \tag{10.44}$$

with R_∞ given by eq. (10.42) and

$$R_s \equiv \frac{(1-\overline{\mu})^2}{1 + \overline{\mu}\mu_s(4 - \overline{\mu}^2)}, \tag{10.45}$$

where $\overline{\mu}$ is an average cosine of the radiance distribution in the asymptotic regime and is expressed through absorption and backscattering coefficients by eq. (10.43), and μ_s is a cosine of the direction of solar rays just below the sea surface:

$$\mu_s = \sqrt{1 - \left(\frac{\sin Z_s}{n_w}\right)^2} \geq \sqrt{1 - 1/n_w^2} \approx 0.6656; \tag{10.46}$$

here Z_S is the solar zenith angle, and n_w is the water refractive index.

The ratio of direct irradiance to the diffuse irradiance just below the water surface q_w can be expressed through the similar ratio measured just above the water surface q_a through the following expression [91]:

$$q_w = \frac{(1-f)T_\downarrow^S q_a}{f(1-A_f) + (1-f)(1-q_a)T_\downarrow^D + a_q T_\downarrow^S}, \tag{10.47}$$

here A_f is a foam albedo, f is a fraction of the water surface covered by white caps that can be estimated from the wind speed u using the following empirical equation [91]:

$$f = \begin{cases} 1.2 \cdot 10^{-5}\, u^{3.3}, & u \leq 9\,\mathrm{m\,s^{-1}}, \\ 1.2 \cdot 10^{-5}\, u^{3.3}(0.221u - 0.99), & u > 9\,\mathrm{m\,s^{-1}}. \end{cases} \tag{10.48}$$

The transmittance of direct solar light penetrated to water depth through the wind roughened surface was computed for different wind speeds and solar zenith angles using Monte Carlo modeling of the water surface from an experimentally derived spectrum of wind waves with the results converted to the following equation [91]:

$$T_\downarrow^S(Z_S, u) = 1 - a_0(u) - R_F^0(Z_S)\left\{a_1(u) + R_F^0(Z_S)\left[a_2(u) + a_3(u)R_F^0(Z_S)\right]\right\}, \tag{10.49}$$

where R_F^0 is a Fresnel reflection coefficient of unpolarized light by flat water surface:

$$R_F^0(Z_S) = \frac{1}{2}\left[\left(\frac{\cos Z_S - \sqrt{n_w^2 - \sin^2 Z_S}}{\cos Z_S + \sqrt{n_w^2 - \sin^2 Z_S}}\right)^2 + \left(\frac{n_w^2 \cos Z_S - \sqrt{n_w^2 - \sin^2 Z_S}}{n_w^2 \cos Z_S + \sqrt{n_w^2 - \sin^2 Z_S}}\right)^2\right], \tag{10.50}$$

and coefficients a_0 through a_3 expressed through the wind speed u (in $\mathrm{m\,s^{-1}}$):

$$a_0(u) = 0.001(6.944\,831 - 1.912\,076\,u + 0.036\,584\,33\,u^2), \quad (10.51)$$

$$a_1(u) = 0.743\,136\,8 + 0.067\,978\,7\,u - 0.000\,717\,1\,u^2, \quad (10.52)$$

$$a_2(u) = 0.565\,026\,2 + 0.006\,150\,2\,u - 0.023\,981\,0\,u^2 + 0.001\,069\,5\,u^3, \quad (10.53)$$

$$a_3(u) = -0.412\,808\,3 - 0.127\,103\,7\,u + 0.28\,390\,7\,u^2 - 0.001\,170\,6\,u^3. \quad (10.54)$$

Transmission by diffuse light $T_{\downarrow}^{D}$ is obtained by averaging eq. (10.49) over the sky radiance distribution. For Lambertian sky we have the following equation for diffuse transmittance [91]:

$$T_{\downarrow}^{D}(u) = 1.367 \times 10^{-5}(46.434 - u)(1410 + 20.6u + u^2), \quad 0 \le u < 12\,\mathrm{m\,s^{-1}}. \quad (10.55)$$

For overcast sky (cardioid distribution [4]) we have the following equation for diffuse transmittance [91]:

$$T_{\downarrow}^{D}(u) = 6.123{\times}10^{-6}(59.3{-}u)(2564{+}33.74u{+}u^2), \quad 0 \le u < 12\,\mathrm{m\,s^{-1}}. \quad (10.56)$$

The ratio of direct irradiance to the diffuse irradiance just above the water surface is a function of atmospheric optical properties and can be evaluated using the following equation taken from reference [91]:

$$q_a = \left(1 + \frac{B_a \tau_a}{\cos Z_S}\right) \exp\left(-\frac{\tau_a}{\cos Z_S}\right), \quad (10.57)$$

where B_a is a probability of backscattering in atmosphere, and τ_a is a total atmospheric optical thickness.

Equation (10.44) for diffuse reflectance coefficient R, with values of, a, b_B, and q_w measured experimentally, was tested by E. I. Afonin [102] using *in situ* measurements in the waters of Black Sea during the whole light day. The difference between predicted and measured values of R was in the range of 5%.

10.9 Diffuse reflection coefficient of shallow water body illuminated by diffuse light

The diffuse reflection coefficient of a shallow water basin should take into account not only multiple scattering of light inside the water, but multiple reflection of light from the bottom and the surface. For coastal waters it is very important that the model used to derive the DRC is valid not only for arbitrary depth but also for any arbitrary value of inherent optical property thus covering very clear and very turbid shallow water bodies.

According to reference [99] the diffuse reflection coefficient of shallow water with the bottom depth z_B and bottom albedo A_B could be expressed as:

$$R = \frac{R_\infty(1 - A_B R_0) + (A_B - R_\infty)e^{-\alpha_R z_B}}{(1 - A_B R_0) + (A_B - R_\infty)R_0 e^{-\alpha_R z_B}}, \quad (10.58)$$

with

$$R_0 = \left(\frac{2+\overline{\mu}}{2-\overline{\mu}}\right) R_\infty, \quad \alpha_R = 2\overline{\mu}(a+b_B), \tag{10.59}$$

and R_∞ and $\overline{\mu}$ are given, respectively, by eqs (10.42) and (10.43).

Equation (10.58) satisfies all limiting conditions implied by the correct physics of light scattering:

$$R\big|_{z_B\to\infty} \equiv R\big|_{A_B=R_\infty}, \quad R\big|_{z_B=0} = A_B, \quad R\big|_{x_G=0} = 0, \quad R\big|_{x_G=1} = 1. \tag{10.60}$$

Equation (10.58) can be used in algorithms to restore water depth and bottom albedo from remotely measured multispectral optical images of water basins in the cases when the combined nature of the illumination of water surface could be neglected.

10.10 Diffuse attenuation coefficient

Downward and upward diffuse attenuation coefficients of light at depth z are defined as follows:

$$k_d(z) = -\frac{1}{E_d(z)}\frac{\mathrm{d}E_d(z)}{\mathrm{d}z}, \quad k_u(z) = -\frac{1}{E_u(z)}\frac{\mathrm{d}E_u(z)}{\mathrm{d}z}, \tag{10.61}$$

where E_d and E_u are downward and upward irradiances. In the framework of self-consistent approximation diffuse attenuation coefficients for optically deep water can be written as follows [101]:

$$k_d(z) = \alpha_\infty \frac{1 + q_w\left\{\mu_0\varepsilon(z)/\mu_s + hR_s[(2+\overline{\mu}) + 1/\mu_s]Y_s(z)\right\}}{1 + q_w\left\{\varepsilon(z) + hR_s[(2+\overline{\mu}) + 1/\mu_s]F_s(z)\right\}}, \tag{10.62}$$

$$k_u(z) = \alpha_\infty \frac{R_\infty + q_w R_s\left\{\mu_0\varepsilon(z)/\mu_s + h[(2-\overline{\mu}) - 1/\mu_s]Y_s(z)\right\}}{R_\infty + q_w R_s\left\{\varepsilon(z) + h[(2-\overline{\mu}) - 1/\mu_s]F_s(z)\right\}}, \tag{10.63}$$

where

$$\alpha_\infty = \sqrt{4a(a+2b_B) + \overline{\mu}^2 b_B^2} - \overline{\mu}(a+b_B), \tag{10.64}$$

$$Y_s(z) = \begin{cases} \mu_0\mu_s\frac{1-\varepsilon(z)}{\mu_0-\mu_s} - \mu_0\varepsilon(z), & \mu_s \neq \mu_0, \\ \alpha z - \mu_0, & \mu_s = \mu_0, \end{cases} \tag{10.65}$$

$$F_s(z) = \begin{cases} \left(1 - \exp\left[-\alpha z\left(\frac{1}{\mu_s} - \frac{1}{\mu_0}\right)\right]\right) \Big/ \left(\frac{1}{\mu_s} - \frac{1}{\mu_0}\right), & \mu_s \neq \mu_0, \\ \alpha z, & \mu_s = \mu_0, \end{cases} \tag{10.66}$$

$$\alpha = a + 2b_B, \quad \mu_0 = \frac{1+\overline{\mu}^2}{\overline{\mu}(3-\overline{\mu}^2)}, \quad h = \frac{(1+\overline{\mu})^2}{2(1+\overline{\mu}^2)}, \tag{10.67}$$

$$\varepsilon(z) = \exp\left[-\alpha z\left(\frac{1}{\mu_s} - \frac{1}{\mu_0}\right)\right], \tag{10.68}$$

with parameters R_∞, $\overline{\mu}$, R_s and q_w defined, accordingly, by eqs (10.42), (10.43), (10.45), and (10.47).

At large optical depths both k_d and k_u converge to the diffuse attenuation coefficient in asymptotic regime that is given by Gershun's equation:

$$k_d(z), \quad k_u(z)\big|_{cz\to\infty} \Rightarrow k_\infty, \quad k_\infty = a/\overline{\mu}. \tag{10.69}$$

10.11 Optical models of scattering and absorption of light in natural water

10.11.1 The Kopelevich physical model of elastic scattering

The physical model of elastic scattering was proposed by Kopelevich [94, 103]. The original model also included an absorption part that is now obsolete. The scattering part satisfies contemporary criteria for all parts of marine water bodies excluding shallow coastal areas contaminated with clay and sand particles raised from the bottom. The model was based on the results of *in situ* measurements of inherent optical properties and particle size distributions over during several decades by the Shirshov Institute of Oceanology in the Pacific, Indian and Atlantic Oceans.

The angular scattering coefficient in this model consists of three parts: the angular scattering coefficient of pure water, the angular scattering coefficient of small particles, and the angular scattering coefficient of large particles. The angular scattering coefficients of particles have been derived by the solution of the inverse problem to derive particle size distributions using water samples taken in various regions of the World Ocean. Then angular scattering coefficients were calculated using Mie scattering approach.

The large fraction represents organic particles of phytoplankton and detritus with the density $\rho_L = 1\,\mathrm{g\,cm^{-3}}$ and relative to water refractive index $n_L = 1.03$. The size distribution for the large particle fraction was found to be Junge distribution r^{-v} for $1.3\,\mu\mathrm{m} \le r \le 13\,\mu\mathrm{m}$ with $v = 3$. The small fraction represents terrigenic particles with density $\rho_L = 2\,\mathrm{g\,cm^{-3}}$ and relative refractive index $n_S = 1.15$ [10]. The size distribution for the small particle fraction was found to be represented by three Junge distributions: the Junge distribution with $v = 2.5$ for $0.01\,\mu\mathrm{m} \le r \le 0.05\,\mu\mathrm{m}$, the Junge distribution with $v = 3.5$ for $0.05\,\mu\mathrm{m} \le r \le 0.1\,\mu\mathrm{m}$, and the Junge distribution with $v = 4.5$ for $0.1\,\mu\mathrm{m} \le r \le 1.3\,\mu\mathrm{m}$. The model is represented by the following equation:

$$\beta(\lambda,\vartheta) = \beta_W(\lambda,\vartheta) + \left(\frac{550}{\lambda}\right)^{0.3} \beta_L^K(\vartheta) v_L + \left(\frac{550}{\lambda}\right)^{1.7} \beta_S^K(\vartheta) v_S, \tag{10.70}$$

with the pure water angular scattering coefficient $\beta_w(\lambda,\vartheta)$ computed using eq. (10.17), and the angular scattering coefficients of large $\beta_L^K(\vartheta)$ and small $\beta_S^K(\vartheta)$ particles for $\lambda = 550\,\mathrm{nm}$ given in Table 10.12. The volume concentrations v_L and v_S are given in $\mathrm{cm^3\,m^{-3}}$. To convert them to the conventional concentrations the following relationships are used:

$$C_S = \rho_S v_S, \quad C_L = \rho_L v_L. \tag{10.71}$$

Table 10.12. Components of physical model of light scattering by sea water by O. V. Kopelevich [94] in $\mathrm{m}^{-1}\,\mathrm{ster}^{-1}$; small fraction of suspended matter β_S; large fraction of suspended matter β_L (the volume concentration of each component is $1\,\mathrm{cm}^3\,\mathrm{m}^{-3}$)

angle, °	β_S^K	β_L^K	angle, °	β_S^K	β_L^K
0	5.3	140	45	$9.8 \cdot 10^{-2}$	$6.2 \cdot 10^{-4}$
0.5	5.3	98	60	$4.1 \cdot 10^{-2}$	$3.8 \cdot 10^{-4}$
1	5.2	46	75	$2.0 \cdot 10^{-2}$	$2.0 \cdot 10^{-4}$
1.5	5.2	26	90	$1.2 \cdot 10^{-2}$	$6.3 \cdot 10^{-4}$
2	5.1	15	105	$8.6 \cdot 10^{-3}$	$4.4 \cdot 10^{-5}$
4	4.6	3.6	120	$7.4 \cdot 10^{-3}$	$2.9 \cdot 10^{-5}$
6	3.9	1.1	135	$7.4 \cdot 10^{-3}$	$2.0 \cdot 10^{-5}$
10	2.5	0.2	150	$7.5 \cdot 10^{-3}$	$2.0 \cdot 10^{-5}$
15	1.3	0.05	180	$8.1 \cdot 10^{-3}$	$7.0 \cdot 10^{-5}$
30	0.29	0.0028	b, m^{-1}	1.34	0.312

This model gives very good predictions of the angular scattering coefficient for open oceanic waters and for clean biologically stable waters with no clay or sand particles suspended by the water movement.

10.11.2 Chlorophyll-based model of elastic scattering and absorption

This model was proposed by Haltrin [104]. The scattering part of this model is based on a modified version of the Kopelevich [72, 103] elastic scattering model; the absorption part of the model is taken from works by Pope and Fry [8], Prieur and Sathyendranath [9], Morel [105], and Carder *et al.* [2]. The absorption coefficient in this model is represented as follows:

$$a(\lambda) = a_W(\lambda) + 0.06 a_C^0(\lambda)\big(C_C/C_C^0\big)^{0.602} + a_H^0 C_H \exp(-k_H\lambda) + a_F^0 C_F \exp(-k_F\lambda), \tag{10.72}$$

with $C_C^0 = 1\,\mathrm{mg\,m}^{-3}$, $a_W(\lambda)$, $a_C^0(\lambda)$, a_H^0, a_F^0, k_H, and k_F identical to the values given above in section 10.2. The elastic angular scattering coefficient was a modification of Kopelevich's model given by eq. (10.70):

$$\beta(\lambda,\vartheta) = \beta_W(\lambda,\vartheta) + \left(\frac{400}{\lambda}\right)^{1.7} \frac{\beta_S(\vartheta)}{\rho_S} C_S + \left(\frac{400}{\lambda}\right)^{0.3} \frac{\beta_L(\vartheta)}{\rho_L} C_L, \tag{10.73}$$

$$\left.\begin{aligned} \beta_S(\vartheta) &= (5.5870\,\mathrm{m^2\,cm^{-3}\,sr^{-1}}) \exp\left(\sum_{n=1}^{5} s_n \vartheta^{3n/4}\right), \\ \beta_L(\vartheta) &= (190.027\,\mathrm{m^2\,cm^{-3}\,sr^{-1}}) \exp\left(\sum_{n=1}^{5} l_n \vartheta^{3n/4}\right), \end{aligned}\right\} \tag{10.74}$$

Table 10.13. The coefficients to eqs (10.74) for two basic phase functions and [104]

n	1	2	3	4	5
s_n	$-2.957\,089 \cdot 10^{-2}$	$-2.782\,943 \cdot 10^{-2}$	$1.255\,406 \cdot 10^{-2}$	$-2.155\,880 \cdot 10^{-2}$	$1.356\,632 \cdot 10^{-2}$
l_n	$-1.604\,327$	$8.157\,686 \cdot 10^{-2}$	$-2.150\,389 \cdot 10^{-3}$	$2.419\,323 \cdot 10^{-5}$	$-6.578\,550 \cdot 10^{-8}$

where ϑ is the scattering angle in degrees. The coefficients s_n and l_n in eq. (10.74) are given in Table 10.13.

The model given by eqs (10.72)–(10.74) depends on five different concentrations of dissolved and suspended matter, C_C, C_H, C_F, C_S, and C_L. Using several experimentally derived regressions and with the use of optimization procedure the number of independent concentrations was reduced to one – the concentration of chlorophyll C_C in $\mathrm{mg\,m^{-3}}$. The other four concentrations of dissolved and suspended matter are expressed through the chlorophyll concentration:

$$\left.\begin{aligned} C_H &= 0.19334\, C_C \exp\left[0.12343\left(C_C/C_C^0\right)\right], \\ C_F &= 1.74098\, C_C \exp\left[0.12327\left(C_C/C_C^0\right)\right], \\ C_S &= 0.01739(\mathrm{g/mg}) C_C \exp\left[0.11631\left(C_C/C_C^0\right)\right], \\ C_L &= 0.76284(\mathrm{g/mg}) C_C \exp\left[0.03092\left(C_C/C_C^0\right)\right], \end{aligned}\right\} \tag{10.75}$$

This chlorophyll-based model represents a modification and extension of the Kopelevich model and, like the Kopelevich model, is valid for open ocean and biologically stable coastal waters. The model that covers more turbid waters should include more scattering components related, for instance, to clays and suspended sand.

10.11.3 Empirical model of inherent optical properties

The empirical model of inherent optical properties was proposed by Haltrin [106]. It makes it possible to restore an angular scattering coefficient, diffuse reflection and diffuse attenuation coefficients, and also total, upward and downward average cosines over the radiance distribution of diffuse light through the absorption and attenuation coefficients at one fixed wavelength close to 520 nm. This model is based on experimental measurements by Petzold [75] and Timofeyeva [107]. It was tested using independent measurements of the complete set of inherent properties by Mankovsky [76, 77] and showed good agreement between measured and predicted results.

Given, that we know the values of absorption and attenuation coefficients (a and c) measured, for example, with the AC-9 probe by WetLabs, we can estimate all other optical properties using the following procedure:

(1) We compute a beam scattering coefficient b and a single-scattering albedo (probability of elastic scattering) ω_0 through a and c:

$$b = c - a, \quad \omega_0 = b/c. \tag{10.76}$$

(2) A total average cosine is computed through the single-scattering albedo using the following equation:

$$\overline{\mu} = y\{2.617\,839\,8 + y[-4.602\,418 + y(9.004\,06 + y\{-14.599\,94 + y[14.839\,09 + y(-8.117\,954 + 1.859\,322\,2y)]\})]\}, \quad y = \sqrt{1-\omega_0}. \tag{10.77}$$

(2) We compute upward and downward average cosines using the following equations:

$$\overline{\mu}_d = \frac{1-\overline{\mu}(1-\overline{\mu})^2\left\{0.0326 + \overline{\mu}^2\left[0.1661 + \overline{\mu}^2(0.7785 + 0.0228\overline{\mu}^2)\right]\right\}}{2-\overline{\mu}}, \tag{10.78}$$

$$\overline{\mu}_u = \frac{1-0.987\overline{\mu}(1-\overline{\mu})^2\exp\left(\overline{\mu}^2\left\{8.4423+\left[-15.6605+\overline{\mu}^2(21.882-11.2257\overline{\mu}^2)\right]\right\}\right)}{2-\overline{\mu}}, \tag{10.79}$$

(3) We compute the backscattering probability, B, and the backscattering coefficient, b_B, as follows:

$$B = \frac{(1-\omega_0)(1-\overline{\mu}^2)^2}{2\omega_0\overline{\mu}^2(3-\overline{\mu}^2)}, \quad b_B = bB. \tag{10.80}$$

(4) We compute the diffuse reflection coefficient using values of the average cosines:

$$R_\infty = \frac{1-\overline{\mu}/\overline{\mu}_d}{1+\overline{\mu}/\overline{\mu}_u}, \tag{10.81}$$

(5) We compute the diffuse attenuation coefficient using Geshun's equation:

$$\overline{k} = \frac{a}{\overline{\mu}} \equiv c\frac{1-\omega_0}{\overline{\mu}}, \tag{10.82}$$

(6) And, finally, we compute the angular scattering coefficient using the following equation:

$$\beta(\vartheta) = l_0^{-1}\exp\left[q\left(1+\sum_{n=1}^{5}k_n\vartheta^{\frac{n}{2}}\right)\right], \tag{10.83}$$

here ϑ is a scattering angle in radians, $l_0 = 1\,\mathrm{m}$. Coefficients q and k_n ($n = 1,\ldots,5$) are given by the following regressions:

$$\left.\begin{aligned} q &= 2.598 + 5.932\sqrt{l_0 b}(2.992 + l_0 b) - 16.722 l_0 b,\\ k_1 &= 5.2077\omega_0 - 8.9924,\\ k_2 &= 17.59 - 10.886\omega_0,\\ k_3 &= 13.098\omega_0 - 19.863,\\ k_4 &= 10.636 - 7.386\omega_0,\\ k_5 &= 1.515\omega_0 - 2.087. \end{aligned}\right\} \tag{10.84}$$

The FORTRAN code that implements this model is published in reference [108].

10.12 Conclusion

The simplified model presented here of absorption, elastic and Raman scattering, and fluorescence is written as a practical tool – to model radiative transfer in real natural waters using either the radiative transfer approach [109] given by eq. (10.1) or the numerical approach based on Monte Carlo or discrete ordinates (Hydrolight [74]). There are certain aspects of scattering, such as Brillouin scattering, scattering by air bubbles, and scattering by turbulent fluctuations of natural water, that are omitted from this chapter because there is not sufficient material in the literature to cover them quantitatively. Other more developed areas are given in a detail that allows for reasonable representative optical modeling of deep and shallow waters with wind-roughened surface.

References

1. Bricaud, A., and A. Morel, 1986, Light attenuation and scattering by phytoplanktonic cells: a theoretical modeling, *Appl. Optics,* **25**, 571–580.
2. Carder, K. L., Stewart R. G., Harvey, G. R., and Ortner P. B., 1989, Marine humic and fulvic acids: their effects on remote sensing of ocean chlorophyll, *Limnol. Oceanogr.*, **34**, 68–81.
3. Hoepfner, N., and S. Sathyendranath, 1992, Bio-optical characteristics of coastal waters: absorption spectra of phytoplankton and pigment distribution in the western North Atlantic, *Limnol. Oceanogr.*, **37**, 1660–1679.
4. Jerlov, N. G., 1976, *Marine Optics*, Elsevier, Amsterdam.
5. Mobley, C. D., 1994, *Light and Water*, (Academic Press, San Diego, CA).
6. Morel, A., 1988, Optical modeling of the upper ocean in relation to its biogenous matter content (Case I waters), *J. Geophys Res.*, **93C**, 749–810.
7. Morel, A., 2001, Bio-optical properties of oceanic waters: A reappraisal, *J. Geophys. Res.*, **106C**, 7163–7180.
8. Pope, R. M., and E. S. Fry, 1997, Absorption spectrum (380–700 nm) of pure water: II. Integrating cavity measurements, *Appl. Optics*, **36**, 8710–8723.
9. Prieur, L., and S. Sathyendranath, 1981, An optical classification of coastal and oceanic waters based on the specific spectral absorption curves of phytoplankton pigments, dissolved organic matter, and other particulate materials, *Limnol. Oceanogr.*, **26**, 671–689.
10. Shifrin, K. S., 1988, *Physical Optics of Ocean Water*, American Institute of Physics, New York.
11. Smith, R. C., and K. S. Baker, 1981, Optical Properties of Clearest Natural Waters, *Appl. Opt.*, **20**, 177–184.
12. Stramski, D., A. Bricaud, and A. Morel, 2001, Modeling of the inherent optical properties of the ocean based on the detailed composition of the planktonic community, *Appl. Optics*, **40**, 2929–2945.
13. Stramski, D., and C. D. Mobley, 1997, Effect of microbial particles in oceanic optics: a database of single-particle optical properties, *Limnol. Oceanogr.*, **42**, 538–549.
14. Babin, M., A. Morel, V. Fournier-Sicre, F. Fell, and D. Stramsky, 2003, Light scattering properties of marine particles in coastal and open ocean waters as related to the particle mass concentration, *Limnol. Oceanogr.*, **48**, 843–859.

15. Morel, A., 1974, Optical properties of pure water and pure sea water, Chapter 1, pp. 1–24, in *Optical Aspects of Oceanography*, eds. N. G. Jerlov, and E. Steemann Nielsen, Academic Press, London.
16. Morel, A., and H. Loisel, 1998, Apparent optical properties of oceanic water: dependence on the molecular scattering contribution, *Appl. Optics*, **37**, 4765–4776.
17. Stramski, D., and D. A. Kiefer, 1991, Light scattering by microorganisms in the open ocean, *Prog. Oceanog.*, **28**, 343–383.
18. Subramaniam, A., E. J. Carpenter, and P. G. Falkowski, 1999, Bio-optical properties of the marine diazotrophic cyanobacteria *Trichodesmium* spp. II. A reflectance model for remote sensing, *Limnol. Oceanogr.*, **44**, 618–627.
19. Subramaniam, A., E. J. Carpenter, D. Karentz, and P. G. Falkowski, 1999, Bio-optical properties of the marine diazotrophic cyanobacteria *Trichodesmium* spp. I. Absorption and photosynthetic action spectra, *Limnol. Oceanogr.*, **44**, 608–617.
20. Ulloa, O., S. Sathyendranath, T. Platt, and R. A. Quiñones, 1992, Light scattering by marine heterotopic bacteria, *J. Geophys. Res.*, **97 C**, 9619–9629.
21. Voss, K. J., W. M. Balch, and K. A. Kilpatrick, 1998, Scattering and attenuation properties of *Emiliania huxleyi* cells and their detached coccoliths, *Limnol. Oceanogr.*, **43**, 870–876.
22. Waltham, C., J. Boyle, B. Ramey, and J. Smit, 1994, Light scattering and absorption caused by bacterial activity in water, *Appl. Optics*, **33**, 7536–7540.
23. Bartlett, J. S. , K. J. Voss, S. Sathyendranath, and A. Vodacek, 1998, Raman scattering by pure water and seawater, *Appl. Optics,* **37**, 3324–3332.
24. Bartlett, J. S., 1997, A comparison of models of sea-surface reflectance incorporating Raman scattering by water, in *Ocean Optics XIII: SPIE,* 2963, S. G. Ackleson and R. Frouin (eds), Bellingham, WA, pp. 592–596.
25. Berwald, J., D. Stramski, C. D. Mobley, and D. Kiefer, 1998, Effect of Raman scattering on the average cosine and diffuse attenuation coefficient of irradiance in the ocean, *Limnol. Oceanogr.*, **43**, 564–576.
26. Desidero, R. A., 2000, Application of the Raman scattering coefficient of water to calculations in marine optics, *Appl. Optics*, **39**, 1893–1894.
27. Faris, G. W., and R. A. Copeland, 1997, Wavelength dependence of the Raman cross section for liquid water, *Appl. Optics*, **36**, 2686–2688.
28. Gordon, H. R., 1999, Contribution of Raman scattering to water-leaving radiance: a reexamination, *Appl. Opt.*, **38**, 3166–3174.
29. Haltrin, V. I., and G. W. Kattawar, 1991 Effects of Raman scattering and fluorescence on apparent optical properties of seawater, Report, Department of Physics, Texas A&M University, College Station, TX.
30. Haltrin, V. I., and G. W. Kattawar, 1993, Self-consistent solutions to the equation of transfer with elastic and inelastic scattering in oceanic optics: I. Model, *Appl. Optics*, **32**, 5356–5367.
31. Haltrin, V. I., G. W. Kattawar and A. D. Weidemann, 1997, Modeling of elastic and inelastic scattering effects in oceanic optics, in *Ocean Optics XIII, SPIE,* 2963, S. G. Ackleson and R. Frouin (eds), Bellingham, WA, pp. 597–602.
32. Hu, C., and K. J. Voss, 1997, *In situ* measurements of Raman scattering in clear ocean water, *Appl. Optics*, **36**, 6962–6967.
33. Kattawar, G. W., and Xin Xu, 1992, Filling-in of Fraunhofer Lines in the Ocean by Raman Scattering, *Appl. Optics*, **31**, 6491–6500.
34. Marshall, B. R., and R. C. Smith, 1990, Raman Scattering and in-water ocean optical properties, *Appl. Optics*, **29**, 71–84.

35. Romanov, N. P., and V. S. Shuklin, 1975, Raman scattering cross section of liquid water, *Opt. Spectrosc.*, **38**, 646–648.
36. Schrötter, H. W., and H. W. Klöckner, 1979, Raman scattering cross-sections in gases and liquids, (pp. 123–166, in *Raman Spectroscopy of Gases and Liquids*, ed. A. Weber, Springer Verlag, Berlin.
37. Shen, Y. R., and N. Blombergen, 1965, Theory of simulated Brillouin and Raman scattering, *Phys. Rev. A*, **137**, 1787–1805.
38. Stavn, R. H., 1993, The effects of Raman scattering across the visible spectrum in clear ocean water: A Monte-Carlo Study, *Appl. Optics*, **32**, 6853–6863.
39. Stavn, R. H., and A. D. Weidemann, 1988, Optical modeling of clear ocean light fields: Raman scattering effects, *Appl. Optics*, **27**, 4002–4011.
40. Stavn, R. H., and A. D. Weidemann, 1992, Raman scattering in oceanic optics: quantitative assessment of internal radiant emission, *Appl. Optics*, **31**, 1294–1303.
41. Sugihara, S., M. Kishino, and N. Okami, 1984, Contribution of Raman scattering to upward irradiance in the sea, *J. Ocean. Soc. of Japan*, **40**, 397–403.
42. Walrafen, G. E., 1967, Raman spectral studies of the effects of temperature on water structure,, *J. Chem. Phys.*, **47**, 114–126.
43. Walrafen, G. E., 1969, Continuum model of water – an erroneous interpretation, *J. Chem. Phys.*, **50**, 567–569.
44. Waters, K. J., 1995, Effects of Raman scattering on the water-leaving radiance, *J. Geophys. Res.*, **100C**, 13151–13161.
45. Aiken, J., 1989, Investigation of various fluorescence phenomena, Report, Plymouth Marine Laboratory, Plymouth, UK, pp. 1–38.
46. Dirks, R. W. J., and D. Spitzer, 1987, On the radiative transfer in the sea, including fluorescence and stratification effects, *Limnol. Oceanogr.*, **32**, 942–953.
47. Dirks, R. W. J., and D. Spitzer, 1987, Solar radiance distribution in deep natural waters including fluorescence effects, *Appl. Optics*, **26**, 2427–2430.
48. Gordon, H. R., 1979, Diffuse reflectance of the ocean: the theory of its augmentation by chlorophyll *a* fluorescence at 685 nm, *Appl. Opt.*, **18**, 1161–1166.
49. Hawes, S. K., Carder, K. L., and Harvey, G. R. 1992, Quantum fluorescence efficiencies of fulvic and humic acids: effect on ocean color and fluorometric detection, *Ocean Optics XI*, *Proceedings of SPIE*, 1750, pp. 212–223.
50. Kattawar, G. W., and J. C. Vastano, 1982, Exact 1-D solution to the problem of chlorophyll fluorescence from the ocean, *Appl. Optics*, **21**, 2489–2492.
51. Kiefer, D. A., 1973, Fluorescence properties of natural phytoplankton populations, *Mar. Biol.*, **22**, 263–269.
52. Kiefer, D. A., W. S. Chamberlin, and C. R. Booth, 1989, Natural fluorescence of chlorophyll *a*: relationship to photosynthesis and chlorophyll concentration in the western South Pacific gyre, *Limnol. Oceanogr.*, **34**, 868–881.
53. Maritorena, S., A. Morel, and B. Gentili, 2000, Determination of the fluorescence quantum yield by oceanic phytoplankton in their natural habitat, *Appl. Optics*, **39**, 6725–6737.
54. Neville, R. A., and J. F. R. Gower, 1977, Passive remote sensing of phytoplankton via chlorophyll a fluorescence, *J. Geophys Res.*, **82**, 3487–3493.
55. Peacock, T. B., K. L. Carder, C. O. Davis, and R. G. Steward, 1990, Effects of fluorescence and water Raman scattering on models of remote sensing reflectance, *Ocean Optics X*, *Proceedings of SPIE*, 1302, pp. 303–319.
56. Preisendorfer, R. W., 1988, Theory of fluorescent irradiance fields in natural waters, *J. Geophys. Res.*, **93**, 10 831–10 855.

57. Slovacek, R., P. Hannan, 1977, *In vivo* fluorescence determination of phytoplankton chlorophyll *a*, *Limnol. Oceanogr.*, **22**, 919–925.
58. Spitzer, D., and R. W. J. Dirks, 1985, Contamination of the reflectance of natural waters by solar-induced fluorescence of dissolved organic matter, *Appl. Optics*, **24**, 444–445.
59. Traganza, E. D., 1969, Fluorescence excitation and emission spectra of dissolved organic matter in sea water, *Bulletin of Marine Science*, **19**, 897–904.
60. Trees, C., 1990, Frequency shifting of light by fluorescence, Technical Memorandum No. 0005–90, pp. 1–9, SDSU Foundation, Center for Hydro-Optics and Remote Sensing, San Diego, CA.
61. Vodacek, A., 1992, An explanation of the spectral variation in freshwater CDOM fluorescence, *Limnol. Oceanogr.*, **37**, 1808–1813.
62. Vodacek, A., S. A. Green, and N. V. Blough, 1994, An experimental model of the solar stimulated fluorescence of chromophoric dissolved organic matter, *Limnol. Oceanogr.*, **39**, 1–11.
63. Terrill, E. J., W. K. Melville, and D. Stramski, 2001, Bubble entrainment and their influence on optical scattering in the upper ocean, *J. Geophys. Res.*, **106C**, 16 815–16 823.
64. Zhang, X., M. Lewis, and B. Johnson, 1998, Influence of bubbles on scattering of light in the ocean, *Appl. Optics*, **37**, 6525–6536.
65. Zhang, X., M. Lewis, M. Lee, B. Johnson, and G. Korotaev, 2002, The volume scattering function of natural bubble populations, *Limnol. Oceanogr.*, **47**, 1273–1282.
66. Cummings, H. Z., and R. W. Gammon, 1966, Rayleigh and Brillouin scattering in liquids: the Landau–Placzek ratio, *J. Chem. Phys.*, **44**, 2785–2797.
67. Goldblatt, N., 1969, Stimulated Brillouin scattering, *Appl. Optics*, **8**, 1559–1566.
68. Joelson, B., and G. Kattawar, 1996, Multiple scattering effects on the remote sensing of the speed of sound in the ocean by Brillouin scattering, *Appl. Optics*, **35**, 2693–2701.
69. O'Connor, C. L., and J. P. Schlupf, 1967, Brillouin scattering in water: the Landau–Placzek ratio, *J. Chem. Phys.*, **47**, 31–38.
70. Bogucki, D. J., J. A. Domaradzki, D. Stramski, and J. R. Zaneveld, 1998, Comparison of near-forward light scattering on oceanic turbulence and particles, *Appl. Optics,* **37**, 4669–4677.
71. Bogucki, D. J., J. A. Domaradzki, R. E. Ecke, and C. R. Truman, 2004, Light scattering on oceanic turbulence, *Appl. Optics,* **43**, 5662–5668.
72. Kopelevich, O. V., V. V. Rodionov, and T. P. Stupakova, 1987, Effect of bacteria on optical characteristics of ocean water, *Oceanology*, **27**, 696–700.
73. Mobley, C. D., and D. Stramski, 1997, Effect of microbial particles in oceanic optics: methodology for radiative transfer modeling and example simulations, *Limnol. Oceanogr.*, **42**, 550–560.
74. Mobley, C. D., and L. K. Sundman, 2000, *Hydrolight 4.1 User Guide,* Sequoia Scientific, Inc., Redmond, WA.
75. Petzold, T. J., 1972, Volume scattering functions for selected ocean waters, SIO Ref. 72–78, Scripps Institute of Oceanography, Visibility Laboratory, San Diego, CA.
76. Mankovsky, V. I., and V. I. Haltrin, 2002, Phase functions of light scattering measured in waters of World Ocean and Lake Baykal, – *2002 IEEE International Geoscience and Remote Sensing Symposium and the 24th Canadian Symposium on Remote Sensing Proceedings on CD ROM*, June 24–28, 2002, Toronto, Canada.

Library of Congress Number: 2002 105858, Paper # I2E09_1759. Also published in *Geoscience and Remote Sensing Symposium*, 2002 IEEE International, IEEE 2002; softcover, 2002: ISBN 0-7803-7536-X; Product No.: CH37380-TBR.

77. Mankovsky, V. I., and V. I. Haltrin, 2003, Light scattering phase functions measured in waters of Mediterranean Sea, *OCEANS 2002 MTS-IEEE Proceedings*, Vol. 4, IEEE Catalog Number: 02CH37362C, ISBN: 0-7803-7535-1, pp. 2368–2373, Biloxi, Mississipi, USA, October 29–31, 2002 (CD-ROM). Also published in *OCEANS, 2002 MTS/ IEEE Conference & Exhibition Proceedings*, ISBN 0-7803-7534-3, IEEE Product no. CH37362-TBR (2003).
78. Haltrin, V. I. , M. E. Lee, and O. V. Martynov, 1996, Polar nephelometer for sea truth measurements, pp. 444–450, in *Proceedings of the Second International Airborne Remote Sensing Conference and Exhibition*, Vol. II, San Francisco, CA, (Published by ERIM: ISSN 1076–7924, 1996).
79. Lee, M. E. and M. Lewis, 2003, A new method for the measurement of the optical volume scattering function in the upper ocean, *J. Atmos. Ocean. Technol.*, **20**, 563–571.
80. Lee, M. E., V. I. Haltrin, E. B. Shybanov, and A. D. Weidemann, 2003, Light scattering phase functions of turbid coastal waters measured in LEO-15 experiment in 2000, in *OCEANS 2003 MTS-IEEE Conference Proceedings on CD-ROM*, pp. 2835–2841, San Diego, California, September 22–26, 2003. ISBN: 0-933957-31-9, Holland Enterprises, Escondido, CA.
81. Haltrin, V. I., M. E. Lee, E. B. Shybanov, R. A. Arnone, A. D. Weidemann, V. I. Mankovsky, W. S. Pegau, and S. D. Ladner, 2002, Relationship between backscattering and beam scattering coefficients derived from new measurements of light scattering phase functions, *Ocean Optics XVI CD-ROM*, November 18–22, 2002, Santa Fe, New Mexico, USA. Prepared by the Office of Naval Research, USA.
82. Haltrin, V. I., M. E. Lee, V. I. Mankovsky, E. B. Shybanov, and A. D. Weidemann, 2003, Integral properties of angular light scattering coefficient measured in various natural waters, pp. 252–257 in *Proceedings of the II International Conference Current Problems in Optics of Natural Waters*, ONW'2003, eds Iosif Levin and Gary Gilbert, St. Petersburg, Russia.
83. Haltrin, V. I., 1997, Theoretical and empirical phase functions for Monte Carlo calculations of light scattering in seawater, pp. 509–518 in *Proceedings of the Fourth International Conference Remote Sensing for Marine and Coastal Environments*, Environmental Research Institute of Michigan, Ann Arbor, MI.
84. Oishi, T., 1990, Significant relationship between the backward scattering coefficient of sea water and the scatterance at 120°, *Appl. Optics*, **29**, 4658–4665.
85. Maffione, R. A. and D. R. Dana, 1997, Instruments and methods for measuring the backwardscattering coefficient of ocean waters, *Appl. Optics*, **36**, 6057–6067.
86. Haltrin, V. I., 2002, One-parameter two-term Henyey–Greenstein phase function of light scattering in seawater, *Appl. Optics*, **41**, 1022–1028.
87. Timofeyeva, V. A., 1975, Brightness in the depth regime in a turbid medium illuminated by normally incident rays, *Izvestiya USSR AS, Atmos. Ocean Physics*, **11**, 259–260.
88. Timofeyeva, V. A., 1978, Relationship between light-field parameters and between scattering phase function characteristics of turbid media, including seawater, *Izvestiya USSR AS, Atmos. Ocean Physics*, **14**, 843–848.
89. Timofeyeva, V. A., 1979, Determination of light-field parameters in the depth regime from irradiance measurements, *Izvestiya USSR AS, Atmos. Ocean Physics*, **15**, 774 -776.

90. Ge, Y., H. R. Gordon, and K. J. Voss, 1993, Simulations of inelastic-scattering contributions to the irradiance field in the ocean: variation in Fraunhofer line depths, *Appl. Optics*, **32**, 4028–4036.
91. Haltrin, V. I., 2004, The nature of optical remote sensing coefficient, in *Remote Sensing and Modeling of Ecosystems for Sustainability*, eds by Wei Gao and David R. Shaw, *Proceedings of SPIE,* 5544, pp. 364–371.
92. Lee, Z. , K. L. Carder, S. K. Hawes, R. G. Steward, T. G. Peacock, and C. O. Davis, 1992, Interpretation of high spectral resolution remote sensing reflectance, in *Optics of Air–Sea Interface: Theory and Measurement,* ed. L. Estep, *Proceedings of SPIE*, 1749, pp. 49–64.
93. Morel, A., and L. Prieur, 1977, Analysis of variations in ocean color, *Limnol. Oceanogr.*, **22**, 709–722.
94. Kopelevich, O. V., 1983, Small–parameter model of optical properties of seawater, pp. 208–234 in *Ocean Optics*, Vol. 1: *Physical Ocean Optics*, ed. A. S. Monin, Nauka, Moscow (in Russian).
95. Gate, L. F., 1974, Comparison of the photon diffusion model and Kubelka–Munk equation with the exact solution of the radiative transfer equation, *Appl. Optics*, **13**, 236–238.
96. Haltrin, V. I., 1988, Exact solution of the characteristic equation for transfer in the anisotropically scattering and absorbing medium, *Appl. Optics*, **27**, 599–602.
97. Henyey, L. C., and J. L. Greenstein, 1941, Diffuse radiation in the galaxy, *Astrophys. J.*, **93**, 70–83.
98. Haltrin, V. I. (*aka* V. I. Khalturin), 1985, The self-consistent two-flow approximation of the transport theory of radiation, *Izvestiya USSR AS, Atmos. and Ocean Physics,* **21**, 589–597.
99. Haltrin, V. I., 1998, Self-consistent approach to the solution of the light transfer problem for irradiances in marine waters with arbitrary turbidity, depth and surface illumination: I. Case of absorption and elastic scattering, *Appl. Optics*, **37**, 3773–3784.
100. Haltrin, V. I., and S. C. Gallegos, 2003, About nonlinear dependence of remote sensing and diffuse reflection coefficients on Gordon's parameter, pp. 363–369, in '*Proceedings of the II International Conference Current Problems in Optics of Natural Waters*,' ONW'2003, eds Iosif Levin and Gary Gilbert, St. Petersburg, Russia, 2003.
101. Haltrin, V. I., 1998, Apparent optical properties of the sea illuminated by Sun and sky: case of the optically deep sea, *Appl. Optics*, **37**, 8336–8340.
102. Afonin, E. I., V. L. Vladimirov, B. Piesick, V. A. Urdenko, and G. Zimmermann, 1985, Ship- and coast-borne investigations of optical properties of medium and parameters of light field of the atmosphere–ocean system, (in Russian), pp. 197–198 in Chapter 6 in *Optical Remote Sensing of the Sea and Influence of the Atmosphere*, The Institute for Space Research, Academy of Sciences of The German Democratic Republic, Berlin.
103. Kopelevich, O. V., and O. A. Gushchin, 1978, Statistical and physical models of the light scattering properties of sea water, *Izvestiya USSR AS, Atmos. Ocean Physics*, **14**, 680–684.
104. Haltrin, V. I., 1999, Chlorophyll based model of seawater optical properties, *Applied Optics*, **38**, 6826–6832.
105. Morel, A., 1980, In-water and remote measurement of ocean color, *Boundary–Layer Meteorol.*, **18**, 177–201.

106. Haltrin, V. I., 2000, Empirical algorithms to restore a complete set of inherent optical properties of seawater using any two of these properties, *Canadian J. Remote Sensing*, **26**, 440–445.
107. Timofeyeva, V. A., 1972, Relation between the optical coefficients in turbid media, *Izvestiya USSR AS, Atmos. Ocean Physics*, **8**, 654–656.
108. Haltrin, V. I., 1999, Empirical algorithms to restore a complete set of inherent optical properties of seawater, in *Proceedings of the Fourth International Airborne Remote Sensing Conference and Exhibition/21st Canadian Symposium on Remote Sensing*, 21–24 June 1999, Ottawa, Ontario, Canada, ISSN 1076–7924, Published by ERIM International, Inc., Ann Arbor, MI.
109. Zege E. P., A. P. Ivanov, and I. L. Katsev, 1991, *Image Transfer through a Scattering Medium*, Springer Verlag, New York.

in "Light Scattering Reviews," Alexander A. Kokhanovsky, Editor,
Springer Verlag, Berlin-Heidelberg-New York:
Praxis Publishing, Chichester, UK, 2006
ISBN 3-540--25315-7